RUSSELL, SPENCER A., M.S. Overexpression, Purification, and Characterization of MmgB and MmgC from *Bacillus subtilis* Strain 168. (2008) Directed by Dr. Jason J. Reddick. 57 pp.

For years, developmental biology has been in search of an understanding as to how an organism undergoes cellular differentiation to produce distinct cell types. *Bacillus subtilis* is a bacterial organism that undergoes cellular differentiation during a process known as sporulation. *B. subtilis* is the most studied spore-forming bacterium and is used as a model for cell fate and development.

Without the availability of glucose as the preferred carbon source, *B. subtilis* must turn to other sources of carbon in order to generate the energy needed for the process of sporulation. One operon in its genome that may be devoted to the breakdown of fatty acids for energy during sporulation is the mother cell metabolic gene (*mmg*) operon. This operon consists of *mmgABCDE* and *yqiQ*, all of which are presumably involved in either fatty acid metabolism or the (methyl)citric acid cycle.

Two genes in this operon, *mmgC* and *mmgB* show similarity to acyl-coenzyme A dehydrogenase and β-hydroxyacyl-coenzyme A dehydrogenase, respectively. Both *mmgC* and *mmgB* have been successfully cloned, overexpressed, and purified from *B. subtilis* strain 168. MmgC has also been biochemically characterized and determined to be a short chain acyl-coenzyme A dehydrogenase. Furthermore, MmgC showed specificity toward isobutyryl-coenzyme A over butyryl-coenzyme A. MmgB, on the other hand, did not show any activity for the dehydrogenation of β-hydroxybutyryl-coenzyme A.

OVEREXPRESSION, PURIFICATION, AND CHARACTERIZATION OF MmgB AND MmgC FROM *BACILLUS SUBTILIS* STRAIN 168

by

Spencer A. Russell

A Thesis Submitted to
The Faculty of the Graduate School at
The University of North Carolina at Greensboro
In Partial Fulfillment
of the Requirements for the Degree of
Master of Science

Greensboro
2008

Approved by

_____
Committee Chair

To Marylin Kata-Kulik

APPROVAL PAGE

This thesis has been approved by the following committee of the Faculty of the Graduate School at the University of North Carolina at Greensboro.

Committee Chair _____

Committee Members _____

_____

_____
Date of Acceptance by Committee

_____
Date of Final Oral Examination

ACKNOWLEDGEMENTS

I thank my faculty mentor and friend, Dr. Jason Reddick, for his time, commitment, and enthusiasm toward my research and lifelong goals. I also thank my research committee members, Dr. Gregory Raner and Dr. Alice Haddy, for sharing their knowledge in the classroom and providing advice throughout my academic career.

I thank my family for their mental and financial support, not only in my academic career, but life. And lastly I thank my soon to be wife, Kelly McOmber, and our daughter, Lillian-Briar, for standing by my side through times of trial and tribulation.

TABLE OF CONTENTS

Page

LIST OF FIGURES

Page

CHAPTER I

INTRODUCTION

I.A Sporulation in *Bacillus subtilis*

Bacillus subtilis is an aerobic, endospore-forming, rod shaped bacterium that is the best-characterized member of the Gram-positive bacteria. They are commonly found in soil, water, and in association with plants. Since *Bacillus* strains have a great capacity to secrete large amounts of enzymes, they are important to the environment, medicine, and industry[1].

The *Bacillus* genome consists of 4,214,810 base pairs, which comprise 4,100 protein coding sequences (CDSs).[1] These 4,100 CDSs comprise 87% of the genome sequence and each CDS has an average size of 890 base pairs.[1] Fifty-eight percent of the *B. subtilis* gene products have been assigned based on significant counterpart.[1] This leaves forty-two percent of the gene products that cannot be assigned a function based on sequence homology alone.

A large portion of the *B. subtilis* genome is devoted to the utilization of a variety of different carbon sources. However, when faced with nutritional starvation, *B. subtilis* initiates responses to restore growth by increasing metabolic diversity. These responses can include the induction of flagellar motility to seek out new food sources through chemotaxis, the production and excretion of macromolecular hydrolases, including proteases and carbohydrases to scavenge any extracellular proteins and polysaccharides,

the production of antibiotics to kill any competing microbes, and the induction of competency for the uptake of exogenous DNA for consumption.[1, 2] If the above responses, invoked through nutritional starvation, prove inadequate, the cells are induced into a process known as sporulation, resulting in the formation of spores. Spores are small metabolically inactive cells that are resistant to heat, desiccation, radiation, and chemical insult.[2]

Sporulation involves a perturbation of the normal cell cycle and the differentiation of a binucleate cell into two cell types[1]. The two cell types include a forespore and a mother cell; each containing an entire copy of the chromosome. Entry into sporulation involves the formation of an axial filament.[3] The axial filament consists of two copies of the chromosome that stretch along the entire length of the cell.[4] A septum is formed next and is located at a polar position.[3] After septation, the forespore becomes engulfed by the mother cell[3] and becomes a free-floating protoplast within the mother cell.[4] At this time, the forespore is now referred to as an endospore and is only encased by two membranes. Through another series of biosynthetic and morphological stages, the endospore is protected with a germ cell wall and cortex, a spore coat, and other protective layers of protein.[4] After this maturation process, the mother cell is lysed and the mature spore is released. A schematic of spore formation can be seen in Figure 1.

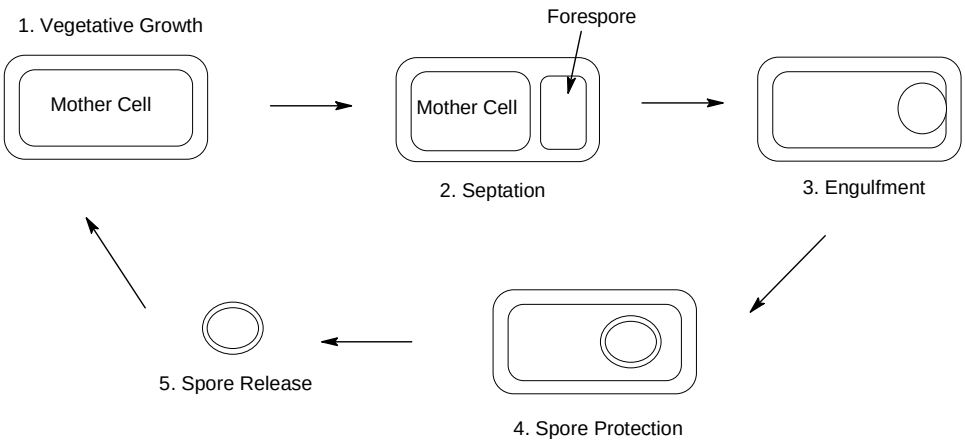

Figure 1. Sporulation of *Bacillus subtilis*. See text for a description of the events taking place during sporulation.

I.B Sigma Factors Involved in Sporulation

In bacteria, there is only one RNA polymerase responsible for the transcription of all RNA.[5] The core of the RNA polymerase is a multi-subunit enzyme, consisting of $\alpha_2\beta\beta'\omega$.[6] Although the core RNA polymerase itself is capable of synthesizing RNA, it is able to recognize specific promoter regions on DNA with the binding of a σ subunit.[7] Specific gene recognition allows for the control of sporulation, as different subsets of genes are spatially and temporally regulated so that expression occurs not only in the correct compartment but also at the correct time in development.[8] During the sporulation process, there is a sequential activation of different σ subunits of RNA polymerase. Each σ factor is then responsible for gene recognition by RNA polymerase. The particular genes that are transcribed are then ultimately responsible for the series of morphological changes that results in sporulation. The different σ factors activated throughout

sporulation include A,H,E,F,G, and K,[9] and the time of their activation is illustrated below in Figure 2.

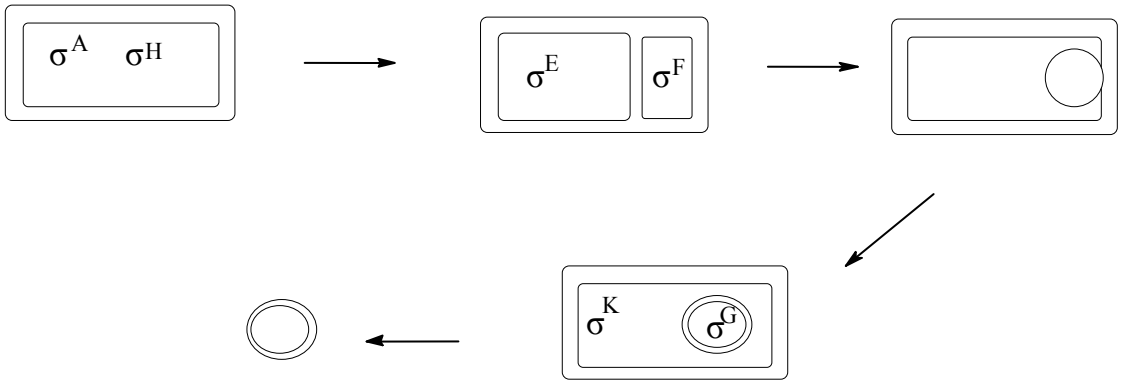

Figure 2. Sigma Factor Activation. A schematic showing the relative activation times of the different sigma factors during sporulation. See Fig 1. for a description of the events during sporulation.

The entire process of sporulation contains a "complex network of interconnected regulatory pathways and developmental checkpoints."[1] However, it is known that the initiation of sporulation ultimately depends on the Spo0A transcription factor; a typical 'response regulator' component of the two component signaling systems that are prevalent in bacteria.[2] The activity of the response regulator is dependent on phosphorylation, which is induced during nutritional starvation, increased cell density, and other cell cycle signals. An elevated level of Spo0A induces sporulation by activating the transcription factors σ^A and σ^H.[9]

σ^A and σ^H appear during vegetative growth and are required for the initiation of sporulation.[9,10] σ^A and σ^H direct the transcription of genes whose products direct the

septum formation to the polar position.[9] σ^A and σ^H are also responsible for the partitioning of a chromosomal copy in the mother cell as well as the forespore.[9]

σ^E and σ^F are synthesized in the predivisional sporangium, however, they do not become active until polar division.[11] σ^E is activated specifically in the mother cell following asymmetric septation.[4, 9] Furthermore, σ^E is first synthesized in its inactive state, pro-σ^E. In response to a signal from the prespore,[4] it is activated by proteolytic cleavage of 27-29 residues from the N-terminus of pro- σ^E.[9, 12] This is the first sign of communication between the mother cell and prespore during sporulation.[4] The removal of the N-terminal domain of the peptide is under the control of the integral protein SpoIIGA.[11] After septum formation, σ^F becomes active in the forespore, while σ^E becomes active in the mother cell.[9, 11] σ^E and σ^F can be attributed to the dissimilar fates of the forespore and the mother cell.[11] The products of the genes regulated by σ^E and σ^F are responsible for the engulfment of the forespore into the mother cell.

Once engulfed, σ^G becomes active in the forespore and its genes are responsible for the preparation of the chromosome for protection and germination.[9] After σ^G activation, σ^K becomes active in the mother cell, and together with σ^E, the forespore is provided with a cortex and several coat proteins.[9] σ^K is also believed to be responsible for genes involved in the lysis of the mother cell, releasing the mature spore.[9]

The sigma factors involved in the sporulation of *B. subtilis* control many genes within its genome and allow it to undergo this biotransformation. However, many of the genes under the control of these sigma factors are not known with complete certainty and many of the proposed functions are based on sequence homology alone. Likewise, many

of the genes show no sequence homology with any understood counterpart and cannot be assigned any function. The sporulation of *B. subtilis* is very complex and little is known about how all the genes biochemically contribute to the sporulation process.

I.C The Mother Cell Metabolic Gene Operon

Bryan, et al, were able to identify genes expressed at intermediate stages of sporulation by screening for σ^E – dependent promoters.[13] σ^E is in control of 253 genes, which are organized into 157 operons.[14] One operon was shown to drive the expression of six different open reading frames (ORFs). The transcription of the genes that Bryan, et al, found are dependent on the mother-cell-specific sigma factor, σ^E, so the operon was named mother cell metabolic genes (*mmg*).[13] The sequence of the transcription unit revealed six ORFs and the ORFs were named *mmgA*, *mmgB*, *mmgC*, *mmgD*, *mmgE,* and *yqiQ*.[13, 14] The transcription of these genes are regulated by *mmgO* and CcpA.[13] *MmgO* is a 14-base pair (bp) catabolite response element centered 22-bps downstream from the *mmg* transcriptional start site.[13] CcpA is a protein that binds to *mmgO* in order to mediate glucose repression of *mmg* promoter activity.[13] From the work of Bryan, et al, it was shown that *mmgO* is required for glucose repression of the *mmg* promoter during sporulation and that CcpA is required for glucose repression of *mmg* promoter activity; CcpA binds to *mmgO* in order to regulate *mmg* promoter activity. ***Knowing this, it seems logical that the genes in this operon may be related to energy production during sporulation because their transcription is regulated in response to carbon source availability.***

Based on sequence homology, the genes of the *mmg* operon can be assigned preliminary functions. The products of *mmgA*, *mmgB*, and *mmgC* are similar to enzymes known to be involved in fatty acid metabolism. *MmgA* is an acetyl-Coenzyme A (CoA) thiolase[15], *mmgB* shows sequence similarity to 3-hydroxybutyryl-CoA (HB-CoA) dehydrogenase, and *mmgC* shows sequence similarity to acyl-CoA (Ac-CoA) dehydrogenase.[13, 14] *MmgD* shows similarity to citrate synthases.[13, 14] *MmgE* shows sequence similarity to 2-methylcitrate dehydratase and *YqiQ* shows greatest similarity to the aldolase, methylisocitrate lyase. **The sequence similarity of these genes to others shows that the mother cell metabolic gene operon may be used in the metabolism of fatty acids for the production of energy during sporulation.**

I.D Fatty Acids and Their Metabolism

The major constituent of bacterial cell membranes is phospholipid. Phospholipids are composed of glycerol-3-phosphate whose C1 and C2 positions are esterified with fatty acids. The properties of the phospholipid depend on the distribution of fatty acids between the 1- and 2- positions on phosphoglycerol and the nature of the phosphate derivative on the 3-position.[16] The physical properties of the fatty acid components also play a significant role in the properties of the phospholipids. The membrane fatty acids can be divided into two major families based on their biosynthetic relationship. The first is the straight-chain fatty acid family and the other is the branched-chain fatty acid family.[17] The straight-chain fatty acids are most common in bacteria, however, the occurrence of branched-chain fatty acids is still significant.[17] The branched chain fatty-acids are a major constituent of *B. subtilis'* phospholipids.[16-18] The most common

straight chain fatty acids include palmitic, stearic, oleic, linoleic, and linoletic acid.[16] The major occurrence of terminally methyl-branched fatty acids was first reported in 1960[16] to include 13-methyl-tetradecanoic acid and 15-methylhexadecanoic acid in *Bacillus subtilis*.[19] Since then, several other methyl-branched fatty acids have been isolated from *Bacillus subtilis*.[18] The function of branched-chain fatty acids are considered when determining the substrates used for phospholipid synthesis and the conformation that branched-chain fatty acids contribute to the fluidity of the membrane.[16] The classification of the methyl-branched fatty acids can be grouped into three series based on their biosynthetic relationship. The three series include anteiso, odd-numbered iso, and even-numbered iso.[16] An anteiso methyl-branched fatty acid contains a methyl group on its ω_3 carbon, while an iso methyl-branched fatty acid contains a methyl group on its ω_2 carbon. These iso fatty acids can have either an even or odd number of carbon atoms.

Although fatty acids are an important building block for cellular components, they can also be degraded to provide energy to the organism. The steps in fatty acid metabolism first involve the activation of a fatty acid by creating a thioester linkage to Coenzyme A (CoA) and then the cycling of oxidation, hydration, oxidation, and thiolysis; the latter four steps are known as the β-oxidation of a fatty acid (Figure 3). An acetyl-CoA and an acyl-CoA two carbons shorter than that of the starting acyl-CoA are generated after one round of β-oxidation.

In the first step of β-oxidation, a fatty acid is first oxidized by an acyl-CoA dehydrogenase, forming an enoyl-CoA. Enoyl-CoA formation involves the transfer of electrons to an FAD or an FMN prosthetic group of the acyl-CoA dehydrogenase,

forming $FADH_2$ or $FMNH_2$, respectively. In the second step, enoyl-CoA is hydrated by an enoyl-CoA hydratase to produce a 3-hydroxyacyl-CoA. The third step is the oxidation of the 3-hydroxyacyl-CoA by a dehydrogenase, with the simultaneous reduction of NAD^+ or $NADP^+$ to form a 3-ketoacyl-CoA and NADH or NADPH, respectively. The final step involves a thiolysis in which the nucleophilic sulphur of CoA-SH attacks the carbonyl of the 3-ketoacyl-CoA to produce acetyl-CoA.

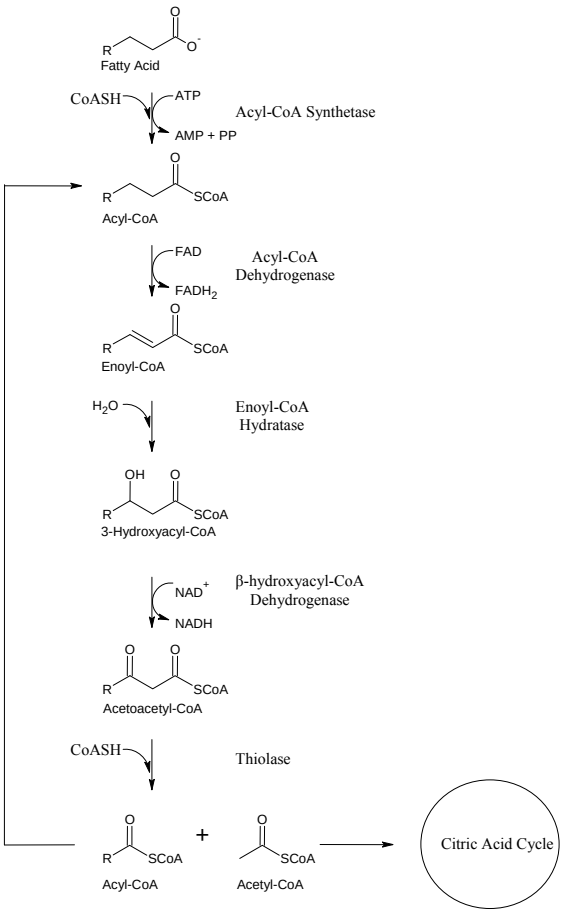

Figure 3. A schematic of fatty acid metabolism. The steps involve first an activation of a fatty acid and then the cycling of oxidation, reduction, oxidation, and thiolysis to produce acetyl-CoA and an acyl-CoA two carbons shorter than that of the starting acyl-CoA. The resulting acyl-CoA re-enters the beta-oxidation cycle.

If the fatty acid is only 4 carbons in length and straight-chained, then one round of β-oxidation would produce 2 acetyl-CoAs. However, if the fatty acid is longer than 4 carbons in length, the thiolysis reaction would only remove a 2-carbon unit from the fatty acid, producing 1 acetyl-CoA and a fatty acid which is 2 carbons shorter in length. β-oxidation would then continue until the entire fatty acid molecule has been converted to acetyl-CoA.

In the event that the fatty acid has an odd number of carbons or is anteiso branched, propionyl-CoA and acetyl-CoA are the ultimate products of β-oxidation. Acetyl-CoA can be used in the citric acid cycle for further energy production through the condensation with oxaloacetate to form citrate (Figure 4). However, when propionyl-CoA is condensed with oxaloacetate, methylcitrate is produced (Figure 4).

By studying mutant strains of *Candida lipolytica,* it was shown that there is a separate pathway for the degradation of odd chain fatty acids.[20] In *E. coli* and *A. nidulans*, there is also a separate regulated pathway in place to oxidize propionate to pyruvate: the methylcitrate cycle.[21, 22] It has also been suggested that propionyl-CoA is converted to succinate and pyruvate through the methylcitric acid cycle in *B. subtilis* (Figure 5).[23] The resulting pyruvate can then be converted to acetyl-CoA by the pyruvate dehydrogenase complex.

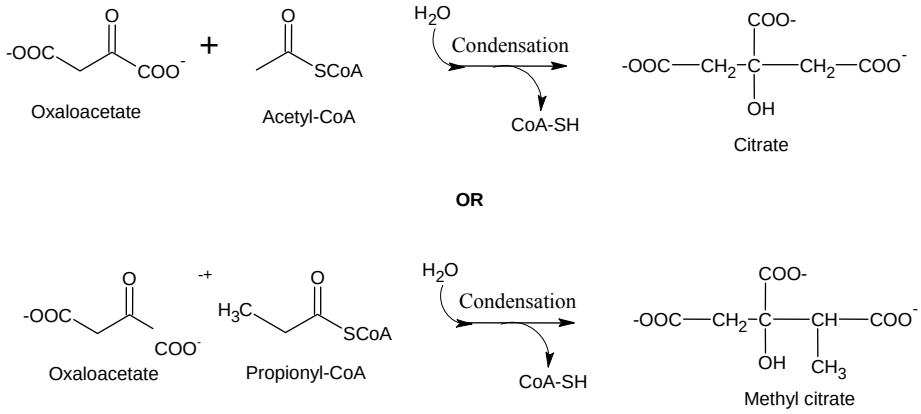

Figure 4. (Methyl)citrate Production. The production of citrate and methylcitrate through a condensation reaction.

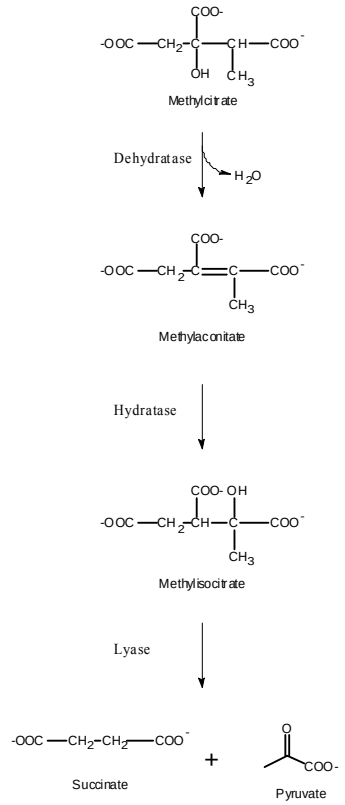

Figure 5. Methylcitric Acid Cycle. Production of succinate and pyruvate from methylcitrate.

Like all metabolic processes, sporulation involves the use of energy. Knowing that sporulation is induced by nutritional starvation and carbon source depravation in *B. subtilis*, the energy required for the sporulation process must be made available through nontraditional metabolic processes. Phospholipids are the major component of bacterial cell membranes and their metabolism can provide an organism with energy during nutritional starvation. The events of fatty acid metabolism are very well studied. However, many of the specific genes in *B. subtilis* responsible for the production of energy during sporulation have not been biochemically characterized. Based on the sequence similarity of the genes found in the mother cell metabolic gene operon to other characterized genes, the σ^E controlled *mmg* operon may contain information on how the energy used during the sporulation process of *B. subtilis* is derived. The goal of this thesis research is to biochemically characterize two of the genes found in the *mmg* operon: *mmgB* and *mmgC*.

CHAPTER II

OVEREXPRESSION AND PURIFICATION OF *MmgC* and *MmgB* FROM *BACILLUS SUBTILIS* STRAIN 168

II.A Introduction to *MmgC* and *MmgB*

During sporulation, the σ^E factor controls the gene expression within the mother cell. Two genes included within the 253 genes under σ^E control are *mmgC* and *mmgB*.[14] Based on the sequence of *mmgC*, it can be classified as an acyl-CoA dehydrogenase,[14, 24] while *mmgB*'s sequence shows similarity to other β-hydroxyacyl-CoA dehydrogenases. Furthermore, both of these genes are conserved in *B. anthracis*, *B. halodurans*, *O. iheyensis*, *C. acetobutylicum*, and *C. perfringens*.[14]

Based on the homology of these genes and their time of activation, it is reasonable to conclude they are involved in the metabolism of fatty acids. After the initial activation of a fatty acid, by the attachment of coenzyme A, the first step in its β-oxidation is its oxidation to an enoyl-CoA by an acyl-CoA dehydrogenase (MmgC). The oxidizing agent typically found in an acyl-CoA dehydrogenase is either FMN or FAD. The fatty acid is then subject to hydration to form a hydroxyacyl-CoA, and then through a subsequent reaction the hydroxyacyl-CoA is dehydrogenated to form a β-ketoacyl-CoA, which is presumably the role of MmgB. Following the dehydrogenation by MmgB is the thiolysis of the acetoacetyl-CoA by MmgA to produce acetyl-CoA and an acyl-CoA.[15]

II.A.1 Goals

The first goal of this research was to clone and over-express *mmgC* and *mmgB*. The second goal was to purify the *mmgC* and *mmgB* proteins. Using the purified protein, the last goal was to characterize the activities of MmgC and MmgB.

In order to clone *mmgC* and *mmgB*, a polymerase chain reaction was performed to produce a large quantity of the gene sequence. After successful PCR, the gene was inserted into a host vector. We choose pET-28a as a suitable vector in which to insert the gene. This vector allows overexpression of genes using the bacteriophage T7 promoter and T7 RNA polymerase.[25] A suitable host for this plasmid is the *E. coli* strain BL21(DE3). *E. coli* BL21 has been infected as the λDE3 lysogen. A λDE3 lysogen has a T7 RNA polymerase downstream from a *lac* promoter. The *E. coli* genome already contains a *lac*I gene, which produces a *lac* repressor protein. This *lac* repressor protein inhibits the binding of *E. coli* RNA polymerase to the *lac* promoter region and therefore inhibits the transcription of the T7 gene to produce T7 RNA polymerase. Furthermore, pET-28a also contains the *lac*I gene, making this a high fidelity system. The addition of isopropyl-beta-D-thiogalactopyranoside (IPTG) removes the *lac* repressor protein from the *lac* promoter sequence and allows *E. coli* RNA polymerase to bind. As the region is transcribed, and consequently translated, T7 RNA polymerase is produced. The T7 RNA polymerase produced from the host *E. coli* DNA can then recognize the T7 promoter region of the pET-28a plasmid and transcribe the target gene sequence directly downstream from the promoter region. A schematic of cloning and expression using this system can be seen in Figure 6[25].

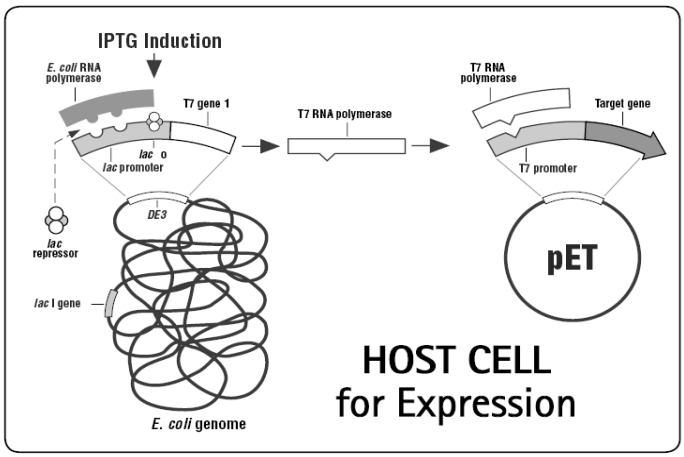

Figure 6. [25] Protein Expression System.

Once *mmgC* and *mmgB* are successfully cloned and overexpressed, the *mmgC* and *mmgB* gene products need to be purified. During the cloning process, six histidine (His_6) residues would have been attached to either the C- or N-terminus of the gene. Because of the His_6 tag present on MmgC and MmgB, QIAGEN's patented nickel-nitrilotriacetic acid (Ni-NTA) metal-affinity chromatography methods can be used to purify the protein from the cell. Nitrilotriacetic acid is a tetradentate chelating agent. The nitrilotriacetic acid can therefore form a chelating complex with a nickel ion. The nickel ion contains a coordination sphere able to bind to six different ligands. Nitrilotriacetic acid would occupy four of these ligand binding sites, leaving two available for interaction with the His_6 -tag on the protein.[26] A drawing of this interaction can be seen in Figure 7[26]. Ni-NTA Agarose is composed of Ni-NTA coupled to Sepharose® CL-6B and is able to bind approximately 5-10 mg of His_6-tagged protein per milliliter of resin.[26] A two milliliter column bed will be used to purify our proteins.

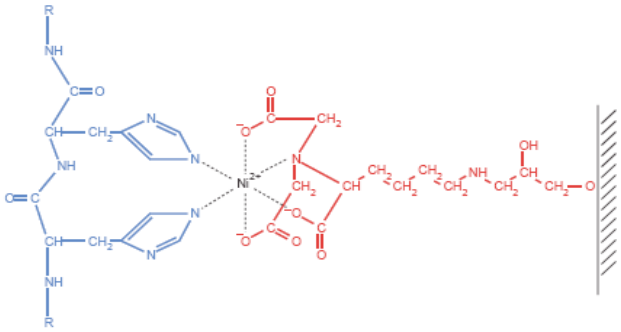

Figure 7. Ni-NTA. The interaction of two histidine residues located on the protein to the Ni-NTA matrix of the column.

The first step in the purification of the protein involves the lysis of the cells. Once the protein is released from the cell, it can be applied to the Ni-NTA column. As the sample moves through the column, the His_6 tagged protein will stick to the column bed. In order to remove proteins of no interest that may have also shown affinity to the column bed, a 60 mM imidazole solution will be passed through the column. Histidine contains an imidazole functional group as shown in Figure 8. The free imidazole will displace the binding of nonspecific histidine residues on unwanted protein. The His_6 tagged protein can then be eluted from the column by further increasing the concentration of imidazole to 200 mM. The imidazole can then be removed from the protein solution through buffer exchange. This will be done by repeat concentration/dilution in an Amicon centriprep 3 filtration unit.

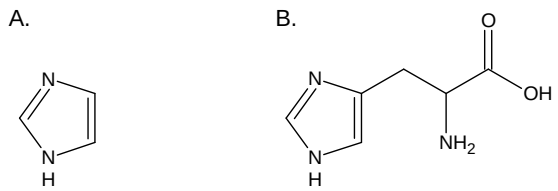

Figure 8. Histidine versus Imidazole. A. Imidazole structure. B. Histidine structure.

Having purified and concentrated protein allows for its biochemical characterization. Acyl-CoA dehydrogenases have been previously characterized from a wide variety of organisms and are responsible for the first, rate limiting step in the β-oxidation cycle of fatty acid metabolism.[27] Also, many of the acyl-CoA dehydrogenases are FAD-linked and deliver reducing equivalents to electron transferring flavoproteins (ETF).[28] Furthermore, Jia Zeng and Ding Li claim that "[A]cyl-CoA dehydrogenases are all homotetramers and each subunit contains 1 mol of FAD.[27]"

One method of acyl-CoA dehydrogenase activity determination involves the use of phenazine methosulfate (PMS) and 2,6-dichlorophenolindophenol (DCPIP). PMS acts as an intermediate electron acceptor and DCPIP act as the terminal electron acceptor for the reaction.[27] The activity of the enzyme can be monitored spectrophotometrically following the decrease in absorbance at 600 nm ($\varepsilon_{600\ nm} = 21\ mM^{-1}\ cm^{-1}$).[27] In studies of mutated rat mitochondrial acyl-CoA dehydrogenase, activity was assayed in the presence of acyl-CoA, phenazine methosulfate (PMS), and 2,6-dichlorophenolindophenol (DCPIP).[27, 29]

Another method for acyl-CoA dehydrogenase activity detection is to follow the reduction of ferricenium ion at 300 nm ($\varepsilon_{300\ nm} = 4.3\ mM^{-1}$).[30] Ferricenium

hexafluorophosphate ($Fc^+PF_6^-$) is an organometallic oxidant and mimics a number of features shown by ETF.[28] It can therefore be used as an alternative oxidant of the acyl-CoA dehydrogenase as it has been used for a number of redox proteins including cytochrome C,[31] spinach plastocyanin,[32] and butyryl-CoA dehydrogenase in *Aspergillus nidulans*.[33] In a study of alternate electron acceptors for a medium-chain acyl-CoA dehydrogenase purified from pig kidney, Lehman and Thorpe were able to show that ferricenium salts are excellent acceptors and can react some 150-fold faster than the widely employed phenazine methosulfate.[28] The ferricenium ion also avoids the necessity of purifying ETF, using mediator dyes, and also exhibits low background rates.[30] Ferricenium hexafluorophosphate is commercially available and can be standardized spectrophotometrically at 617 nm ($\varepsilon = 410\ M^{-1}\ cm^{-1}$).[31]

Hydroxyacyl-CoA dehydrogenase activity has also been assayed using a variety of different methods and conditions. Hydroxyacyl-CoA dehydrogenases have been shown to be either NAD(H) or NADP(H)[34] dependent which provides an easy detection method of activity. Upon reduction of NAD(P) to NAD(P)H, there is an increase in absorbance at 340 nm ($\varepsilon = 6.22\ mM^{-1}\ cm^{-1}$).[34-36] Although there is an easy detection method for the activity of NAD(P) dependent acyl-CoA dehydrogenases, there are a variety of other conditions that must be considered when trying to observe enzyme activity. These include the stereospecificity of the enzyme and the pH of the buffer system.

It has been shown that 3-hydroxyacyl-CoA dehydrogenases can be specific toward one enantiomer or the other, and in some cases nonspecific. For example,

Alcaligenes eutrophus contains a non-stereospecific Acac-CoA reductase.[37] On the other hand, *Clostridium kluyveri,*[38] *Escherichia coli,*[39] and *Clostridium beijerinckii*[34] contain L(+)-specific 3-hydroxyacyl-CoA dehydrogenases. There are also D(-) specific 3-hydroxybutyryl-CoA dehydrogenases like those found in pigeon liver[40] and *Azotobacter beijerinckii,*[41] which are also NADP specific. If stereospecificity of the substrate is not a concern, it is common to follow the reduction of Acac-CoA by monitoring the decrease in A_{340} of NAD(P)H.[34, 42, 43] If the stereospecificity is of concern, the stereospecificity of the enzyme has been previously determined by comparison to the pig heart enzyme which is specific towards the (*S*)-enantiomer.[44,34, 38] Incubating the racemic mixture of 3-hydroxybutyryl-CoA (HB-CoA) with the pig heart enzyme until there is no activity observed removes the (*S*)-enantiomer. The pig heart enzyme can then be removed through filtration. Then, by adding the enzyme of interest to the same reaction mixture, it can be determined if the enzyme is specific toward the (*R*)- isomer by monitoring the formation of excess NAD(P)H.

pH plays an important role in enzyme activity and must be considered when designing an enzyme assay. When studying the properties of 3-hydroxybutyryl-CoA dehydrogenase from *Clostridium beijerinckii*, Colby and Chen used 50 mM buffers of Na-MES for pH 5.0 to 6.5, sodium phosphate for pH 6.5 to 8.0, and Tris-Cl for pH 8.0-9.0.[34] They found that in the HB-CoA forming direction of the reaction, pH of 5.0 showed maximum activity and decreased as the pH was increased to 8.0 with approximately 10 % of activity remaining. In the Acac-CoA forming direction, maximum activity was observed at pH 8.0 for $NADP^+$ and decreased when the pH was

both increased and decreased from that value. Similarly, rat mitochondrial his-tagged short chain 3-hydroxyacyl-CoA dehydrogenase had optimal activity at pH 5 in 0.1 mM phosphate buffer containing 0.1 mM DTT when monitoring the reduction of Acac-CoA.[42] In a study on 3-HB-CoA dehydrogenase in *Clostridium kluyveri*, there was optimal activity at a pH of 6.5 for Acac-CoA reduction with a 14-time slower, but optimal oxidation at pH 9.5.[38] From these studies, it is clear that the HB-CoA forming reaction is optimal in a slightly acidic buffer system and the Acac-CoA forming reaction is optimal in a slightly basic buffering system.

After considering the wide variety of conditions, alternative substrates, and activity detection methods, once enzyme activity has been established, the next goal is to determine the kinetic rate constants of the MmgB and MmgC reactions. The rate of a chemical reaction is dependent on the concentration of substrate and can be explained by the equation[45, 46]

$$E + S \underset{k_{-1}}{\overset{k_1}{\rightleftharpoons}} ES \xrightarrow{k_2} E + P,$$

where enzyme (E) and substrate (S) form an enzyme-substrate complex (ES). The ES then decomposes releasing the product (P) and regenerating the enzyme. The formation of the ES complex is considered to be "fast" and its rate of formation is assumed to be in a steady state.[46]

The MmgB and MmgC reactions are bisubstrate reactions. However, we assume that the concentration of the oxidizing agent is saturating and does not change significantly during the reaction. Doing so allows us to assume that the catalyzed reaction is a first-order process, better called a pseudo-first-order reaction. Because the

reaction is a pseudo-first-order reaction, the above equation allows us to characterize an enzyme by calculating its catalytic efficiency (k_{cat}/K_M) using Eq 1. and K_M. The catalytic efficiency of the enzyme is a measure of the number of catalyzed reactions an enzyme makes per unit time. The maximal velocity (V_{max}) can be calculated from Eq. 2. The maximal velocity of an enzyme occurs at saturating substrate concentrations, which assumes that the enzyme is entirely in ES form. The Michaelis constant (K_M) is calculated using Eq. 3. The Michaelis constant represents the substrate concentration at which the reaction is at half of its maximal velocity. A low K_M value describes an enzyme that has an increased affinity over a particular substrate than if it had a higher value for K_M.

Eq. 1. $$k_{cat} = \frac{V_{max}}{[E]_T}$$ 2. $$v_o = \frac{V_{max}[S]}{K_M + [S]}$$ 3. $$K_M = \frac{k_{-1} + k_2}{k_1}$$

II.B Results and Discussion

II.B.1 MmgC/B Amplification

MmgC and *mmgB* were successfully amplified from the *B. subtilis* strain 168 genome by using a polymerase chain reaction (PCR). The results for *mmgC* amplification are shown by the agarose gel in Figure 9. The pictures of the agarose gels were photographed with a digital camera. As can be seen in all the pictures of the agarose gels experiments, the quality of the image is very low. For clarity, a box has been put around the band of interest. For *mmgC*, it can be seen from the gel that the amplified gene falls between the 1.0 and 1.2 bp standards. This is consistent with its

expected size of 1134 bps. The results for *mmgB* amplification are shown by the agarose gel in Figure 10. The pcr product lies between 0.5 and 1.0 kbs and is consistent with the expected gene length of 732 bps.

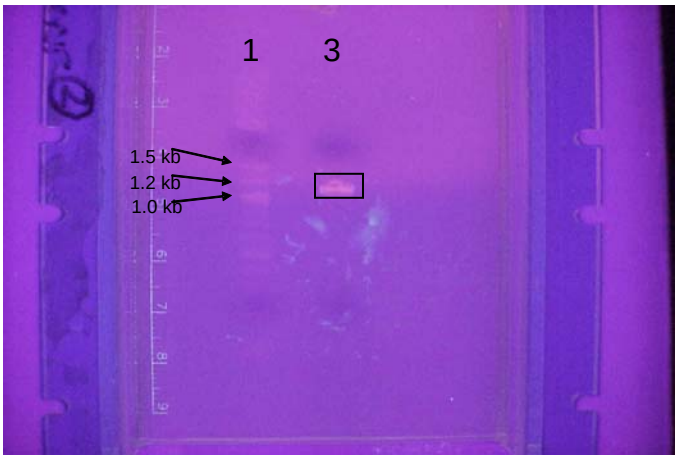

Figure 9. Agarose Gel of PCR Reaction Product of BS168 Genome. Lane 1. Standards. Lane 3. PCR reaction product. The expected size of *mmgC* is 1134 bps.

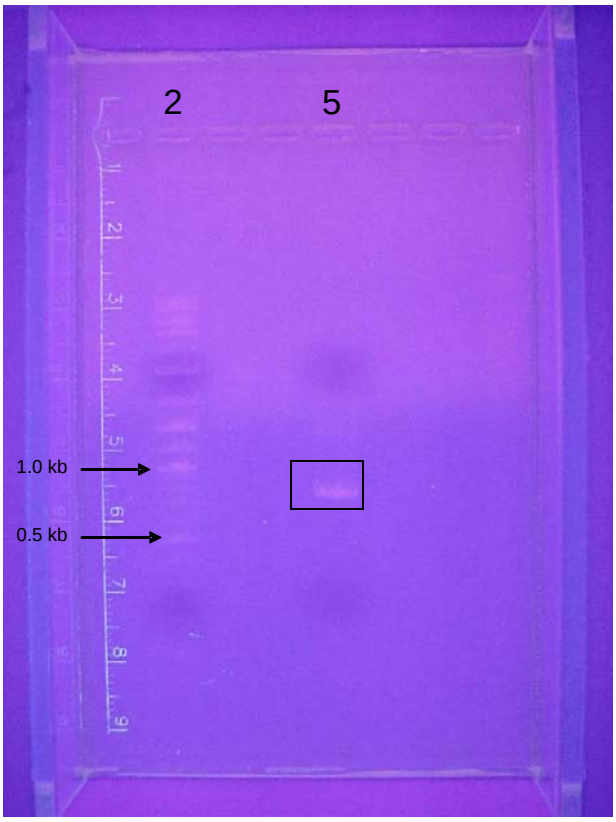

Figure 10. Agarose Gel of PCR Reaction Product of BS168 Genome. Lane 2. Standards. Lane 5. PCR reaction product. The expected size of *mmgB* is 732 bps.

II.B.2 Cloning MmgC/B

MmgC and pET-28a were cut with the restriction enzymes *Xho*I and *Nde*I. Separately, *mmgB* and pET-28a were cut with *Xho*I and *Nco*I. Then, using T4 DNA ligase, *mmgC* and *mmgB* were inserted into the vector, pET-28a. *E. coli* DH5α cells were then transformed using the ligated plasmid, *mmgC*/pET-28a and *mmgB*/pET-28a. Conclusive results of successful ligation and transformation can be seen in the agarose gels in Figure 11 and Figure 12. Purified plasmids from *E. coli* DH5α/*mmgC*/pET-28a and *E. coli* DH5α/ *mmgB*/pET-28a cultures were then used to retransform *E. coli* BL21(DE3).

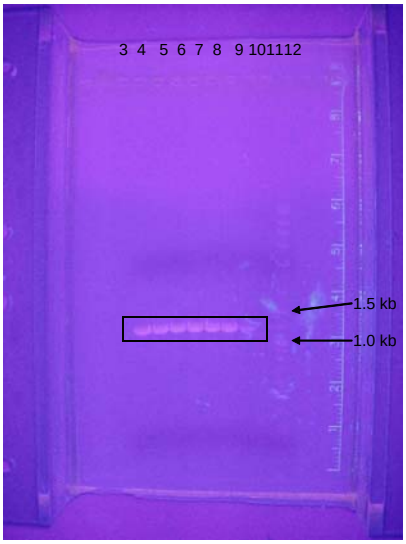

Figure 11. PCR Products of Purified Plasmid from *mmgC*/pET28a/DH5α. Lanes 3,4,5,6,7,8,9: PCR products of the plasmids from transformants. Lane 12: Molecular weight standards. Lane 11: PCR product of pET28a. Lane 10: PCR product of BS168 genomic DNA. The gene length of *mmgC* is 1134 base pairs.

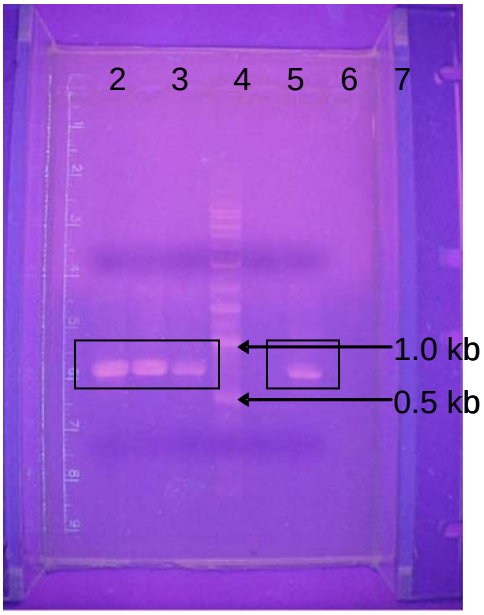

Figure 12. PCR of Purified Plasmid from *mmgB*/pET28a/DH5α. Lanes 2,3,4: Plasmids from three transformants. Lane 5: Molecular weight standards. Lane 6: pET28a. Lane 7: BS168 genomic DNA. The expected size of *mmgB* is 732 bps.

II.B.3 MmgC/B Purification

After successful retransformation into *E. coli* BL21(DE3), MmgC was purified from cultures of BL21(DE3)/MmgC/pET-28a and MmgB was successfully purified from cultures of BL21(DE3)/MmgB/pET-28a using nickel nitrilotriacetic acid column separation. Although incubating BL21(DE3)/MmgB/pET-28a at 37 ^{0}C overnight produced large amounts of protein as observed by SDS-PAGE on whole cell extracts, the protein could not be purified due to inclusion body formation. This was observed on SDS-PAGE by lack of a corresponding protein band after purification (data not shown). In an effort to decrease inclusion body formation and increase the amount of purified protein, incubation was conducted at 18 ^{0}C. The expected molecular weight of MmgC containing a His_6 tag is 41.64 kDa. The expected molecular weight of MmgB containing a His_6 tag is 27.85 kDa. However, this was not consistent with the SDS-PAGE analysis (Figure 13) of purified protein for MmgB. On the gel, MmgB appeared to have a molecular weight of about 31 kDa. Why MmgB did not migrate to its corresponding molecular weight position is unclear. To be sure that the expressed MmgB contained the expected sequence of nucleic acids, it was subjected to DNA sequencing, which is discussed later. Using the methods of Bradford[47] and bovine serum albumin as standard (Figure 14), on average, 2.6 mg of MmgB and 3.8 mg of MmgC was purified per liter of culture.

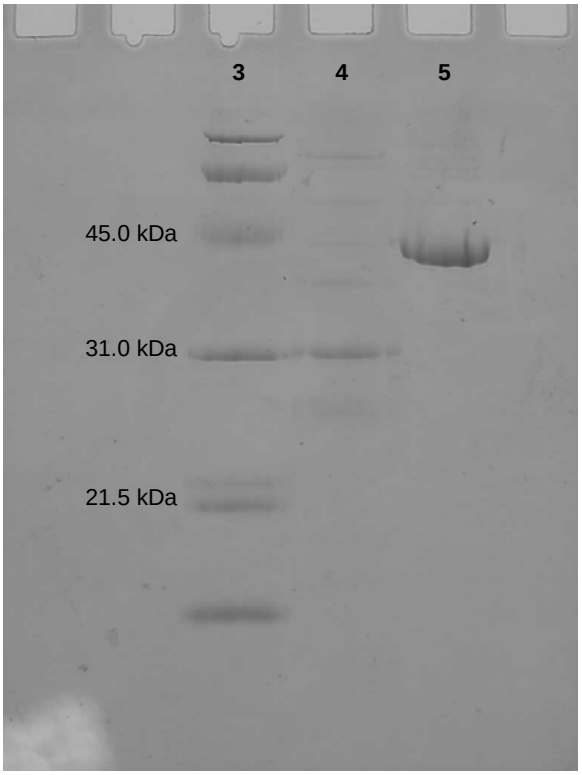

Figure 13. SDS-PAGE of Concentrated Protein After Purification. Lane 3: Molecular weight standards. Lane 4: MmgB. The expected molecular weight of MmgB containing a 6-Histidine tag is 27.85 kDA. Lane 5: MmgC. The expected molecular weight of MmgC containing a 6-Histidine tag is 41.64 kDa.

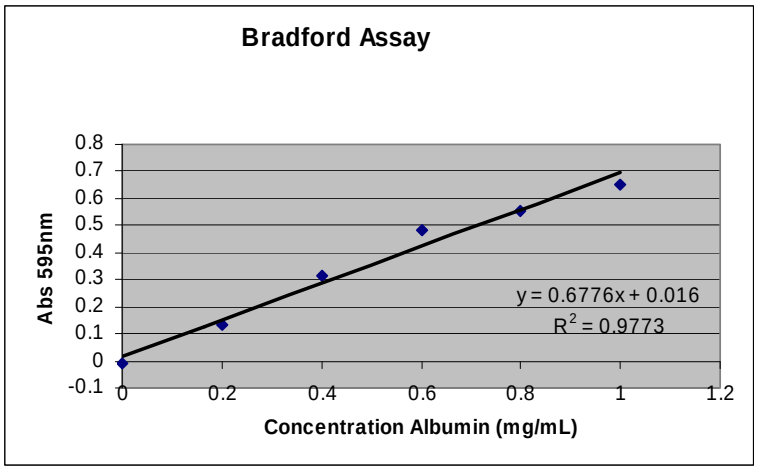

Figure 14. Bradford Assay. Bradford assay using bovine serum albumin as a standard.

II.B.4 Determination of Coenzyme Presence in MmgC and MmgB

Acyl-CoA dehydrogenases are known as either FAD- or FMN- dependent enzymes and the flavins in each have yellow color. When applied to the Ni-NTA column, MmgC appeared yellow. Using MALDI-TOF-MS analysis (Figure 15), it was determined that FAD (Figure 16) was the oxidizing agent present in MmgC.

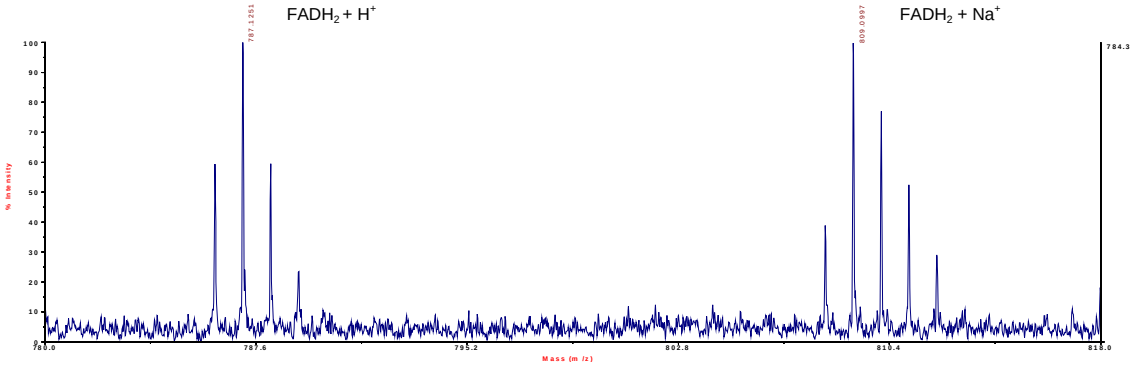

Figure 15. MmgC Coenzyme. MALDI-TOF-MS spectrum of denatured MmgC. The molecular weight of $FADH_2$ is 785.5 a.m.u. The molecular weight of FMN is 478.4 a.m.u.

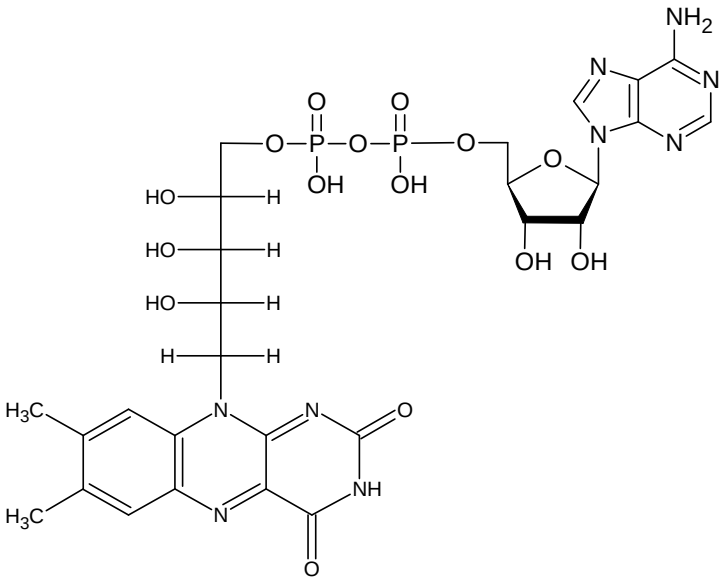

Figure 16. Flavin Adenine Dinucleotide (FAD). FAD is composed of adenosine and ribofloavin attached together by a pyrophosphoryl group.

NADP is a common oxidant utilized by 3-hydroxyacyl-CoA dehydrogenases and furthermore, 3-hydroxybutyryl-CoA dehydrogenases have been shown to be able to utilize either NAD(H) or NADP(H) as a cosubstrate.[34] Using MALDI-TOF-MS analysis, it appears that NADP is likely the preferred oxidizing agent found in MmgB (Figure 17). The spectrum contains many unidentified peaks; however, we assume that the labeled peaks are representative of the presence of NADP.

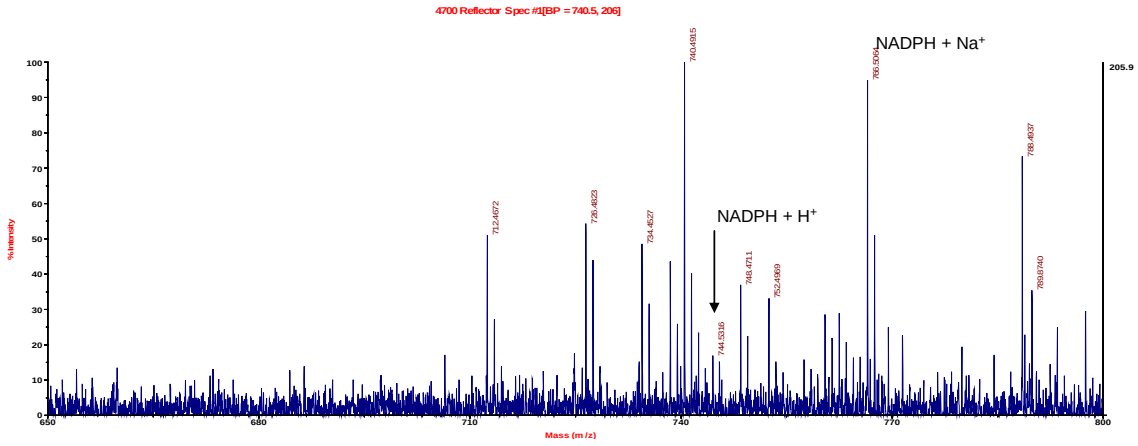

Figure 17. MmgB Coenzyme. MALDI-TOF-MS Spectrum of denatured MmgB showing that NADPH is present.

II.B.5 MmgC Activity Analysis

The purified MmgC was an active enzyme able to convert butyryl-CoA to butenoyl-CoA. The activity was confirmed using MALDI-TOF-MS and HPLC analysis as shown in Figure 18 and Figure 19, respectively. When provided with a different substrate, MmgC was also able to convert isobutyryl-CoA to 2-isobutenoyl-CoA, as observed by MALDI-TOF-MS. However, it did not catalyze the reaction of propionyl-CoA to acrolyl-CoA, or isovaleryl-CoA to 3-methylcrotonyl-CoA. We also propose that MmgC will be able to catalyze the oxidation of 2-methylbutyryl-CoA to 2-methylbutenoyl-CoA, which will be tested after the complete synthesis and purification of this substrate. The reactions discussed above can be seen in Figure 20.

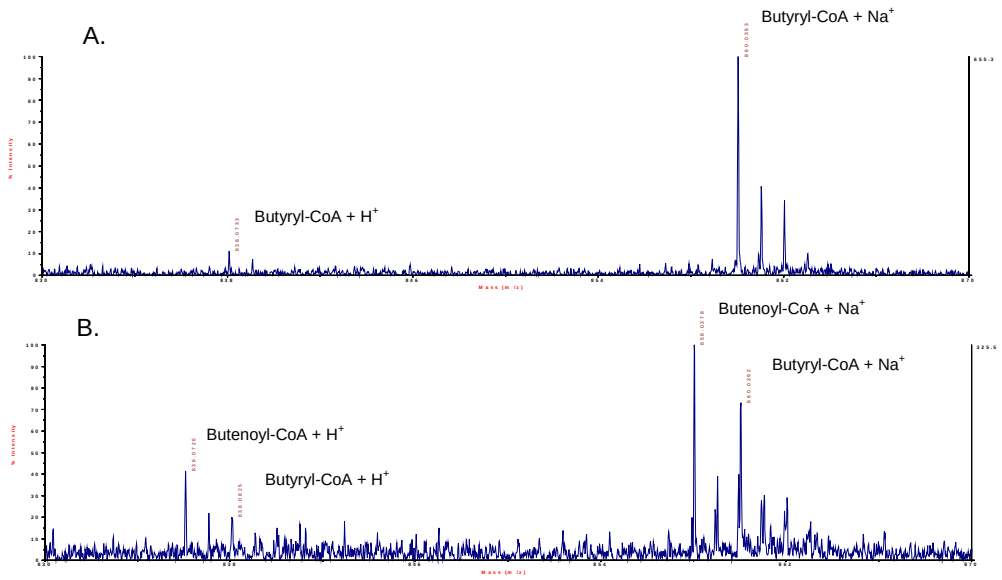

Figure 18. MmgC/Butyryl-CoA Reaction. MALDI-TOF-MS spectra of the MmgC reactions. All peaks are labeled in atomic mass units. A) Reaction mixture lacking MmgC. B) Reaction mixture including MmgC.

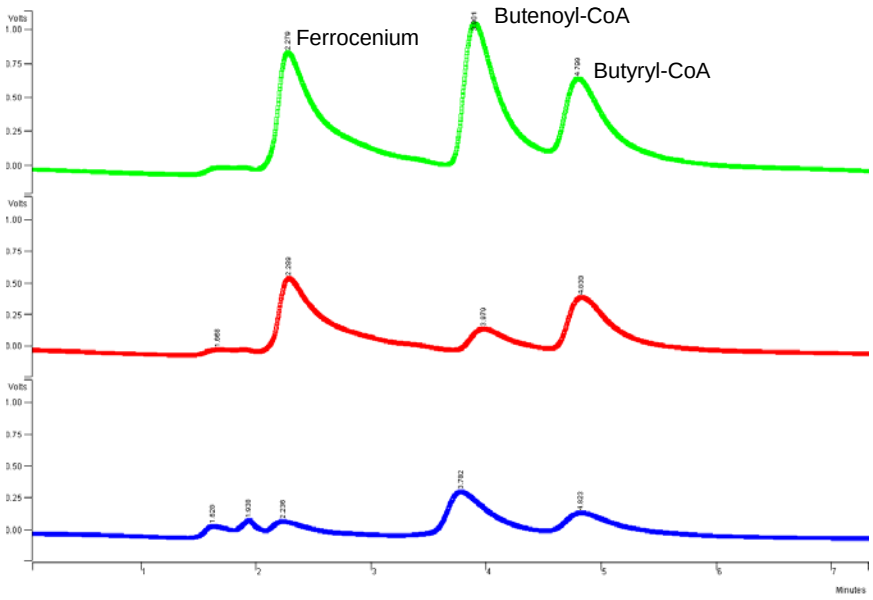

Figure 19. HPLC of MmgC/Butyryl-CoA Reaction. Top: 450 µM Ferricenium Hexafluorophosphate, 200 µM Butyryl-CoA, 200 µM Butenoyl-CoA. Middle: Ferricenium, Butyryl-CoA, and MmgC after an initial incubation of 20 minutes. Bottom: Ferricenium, Butyryl-CoA, and MmgC after an incubation time of 2 hours.

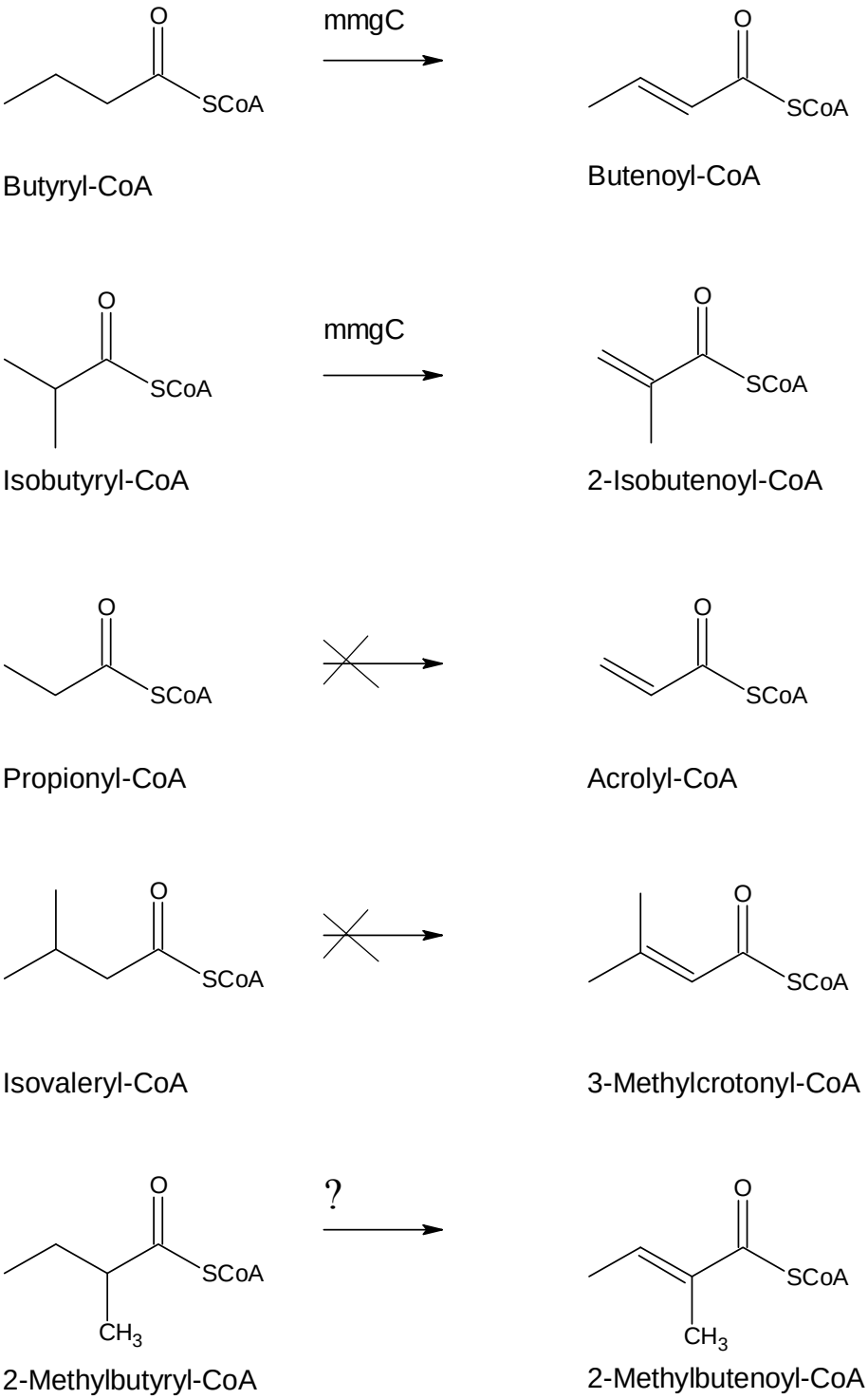

Figure 20. Proposed MmgC Reactions. MmgC represents an observed reaction. An X represents a reaction that was not observed. A ? denotes a reaction not studied.

II.B.6 MmgC Kinetic Analysis

MmgC has shown activity against both butyryl-CoA and isobutyryl-CoA. Kinetic analysis of the mmgC reactions have an apparent k_{cat} for MmgC against butyryl-CoA to be 6.3 x 10^{-2} s^{-1} with a k_{cat}/ K_M value of 4.5 x 10^2 $M^{-1}s^{-1}$ The apparent k_{cat} for MmgC against isobutyryl-CoA was calculated to be 1.1 x 10^{-1} sec^{-1} with a k_{cat}/ K_M of 1.1 x 10^3 $M^{-1}s^{-1}$. The Michaelis-Menten plot of the reactions can be seen in Figure 21.

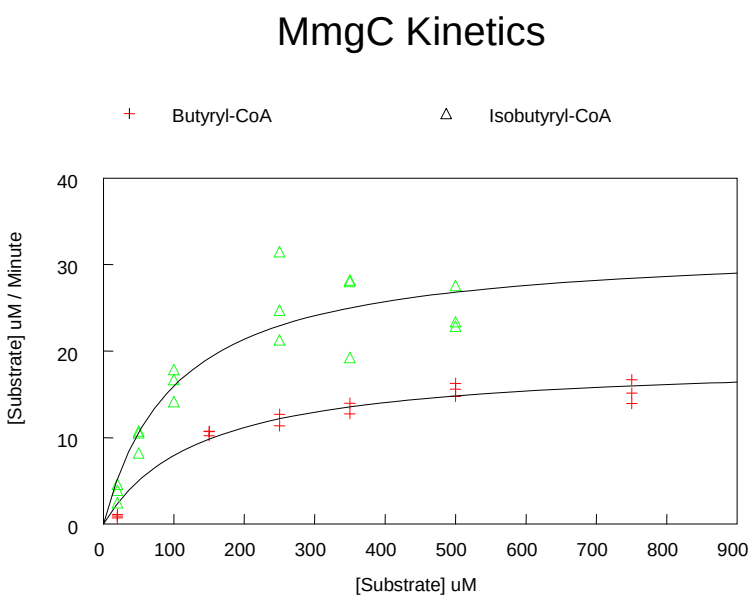

Figure 21. MmgC Kinetic Plot. Michaelis-Menten Plot of MmgC Reactions.

II.B.7 MmgB Kinetic Analysis

MmgB did not catalyze the conversion of DL-β-hydroxybutyryl-CoA, D-β-hydroxybutyryl-CoA, or L-β-hydroxybutyryl-CoA to acetoactetyl-CoA. In the event that pH or buffer salts were inhibiting enzyme activity, several different buffer systems were tried; none of which proved adequate for enzyme activity. Furthermore, because $NADP^+$ and NAD^+ can both act as electron acceptors for β-hydroxyacyl-CoA oxidation, both coenzymes were provided in reaction mixtures; neither of which proved adequate to increase enzyme activity. Likewise, MmgB did not catalyze the conversion of acetoacetyl-CoA to 3-hydroxybutyryl-CoA with either NADH or NADPH provided as coenzyme.

With the possibility of acetoacetyl-CoA exhibiting feedback inhibition towards MmgB, a reaction mixture was also made in the presence of MmgA. MmgA is a thiolase,[15] and would reduce the concentration of acetoacetyl-CoA as it is converted to acetyl-CoA. However, neither acetyl-CoA nor acetoacetyl-CoA formation was observed by MALDI-TOF-MS analysis.

In case of isomer inhibition, enantiopure (*R*)- and (*S*)- β-hydroxybutyryl-coenzyme A was synthesized. Neither substrate was converted into the expected product, as observed by MALDI-TOF-MS analysis.

II.B.8 (S)- and (R)-β-Hydroxybutyryl-CoenzymeA Synthesis

Yuan, et al, had previously synthesized (*R*)-3-hydroxybutyryl CoA.[48] By following their work with a few minor differences, (*S*)- and (*R*)-β-hydroxybutyryl-coenzyme A were successfully synthesized. Because the starting material, β-

hydroxybutyric acid, was enantiopure, it was assumed that our product was also enantiopure. In order to undoubtedly conclude that the synthesized substrates were, in fact, enantiopure, polarimetry experiments are needed. Although they were attempted, the purified samples were too dilute to make any conclusion on the enantiopurity. In order to increase the concentration of the sample, larger quantities of reactants would be needed and in an effort to lower expenditures, small amounts of coenzyme A were used. However, if MmgB had shown activity toward an enantiopure substrate, the experiment would have been scaled up in order to prove enantiopurity. The synthesized product was purified using reverse phase HPLC and lyophilization. In order to conclude that β-hydroxybutyryl-coenzyme A had been synthesized, MALDI-TOF-MS analysis was performed. MALDI-TOF-MS analysis showed the presence of an 854 a.m.u analyte (Figure 22), presumably our product.

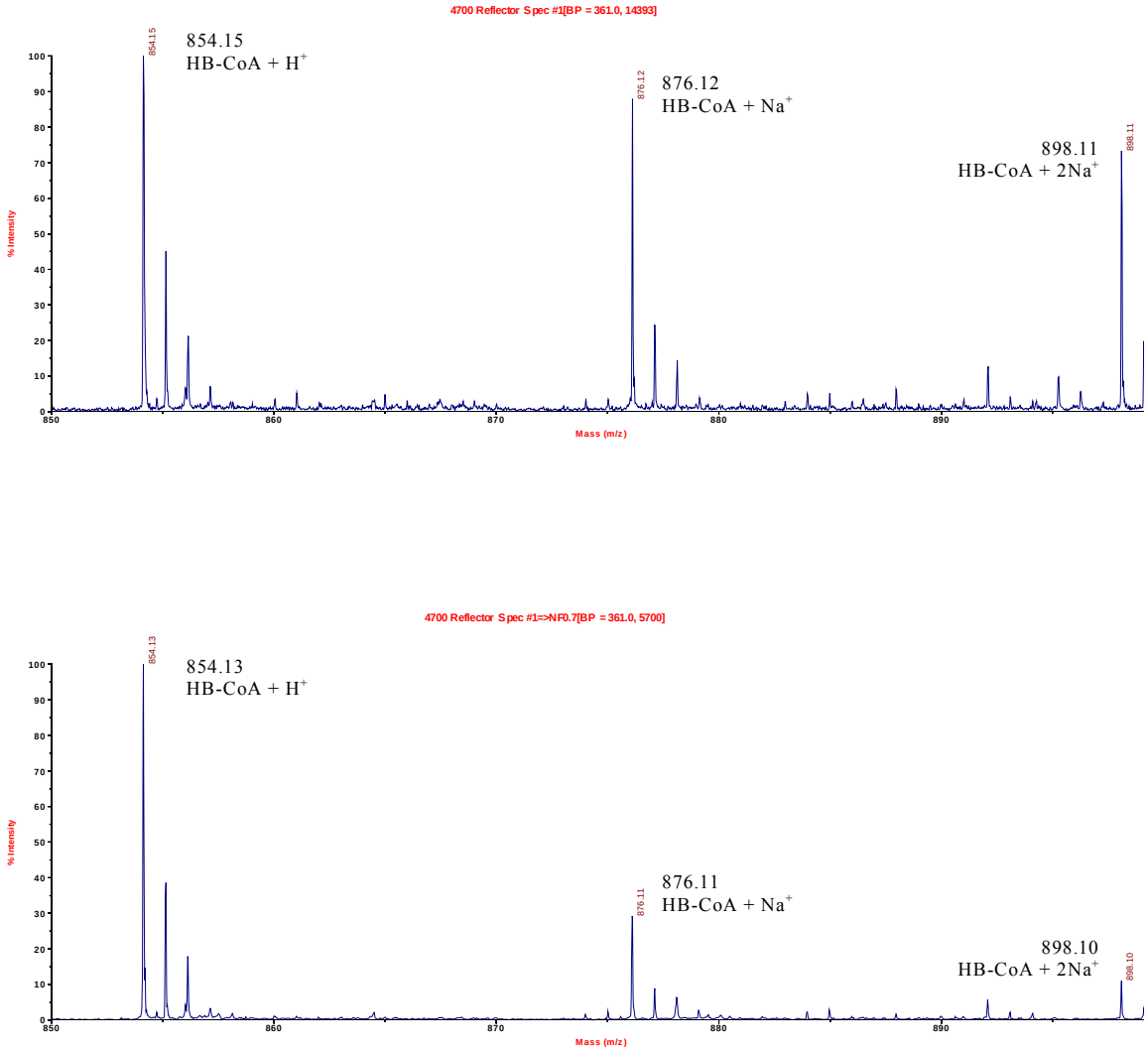

Figure 22. MALDI-TOF-MS analysis of the synthesized (*S*)- and (*R*)- 3-HB-CoAs. The top spectrum is the (*S*)-isomer. The bottom spectrum is the (*R*)-isomer. The expected mass of 3-HB-CoA is 853.6 a.m.u.

II.B.9 MmgB Gene Sequencing

The sequence of MmgB, analyzed by SeqWright DNA Technology Services, Houston, TX was returned and matched the DNA sequence published by Bryan, et al.[13] However, when aligned with the Subtilist genome project data,[24] there were three nucleotides present that do not match the data published by Bryan, et al, (Figure 23). The MmgB sequence published by Bryan, et al, can be found in the NCBI data bank under accession number U29084. The Subtilist genome project lacks a guanine at positions 499 and 504, and also a cytosine at position 505. Although there are differences between the two sequences, the returned sequence was properly in frame with the promoter. However, because the nucleic acids are not located consecutively within the sequence, there is a total difference of three amino acids (Figure 24). According to the Subtilist genome project, the expressed mmgB protein has an arginine residue at position 166 and a threonine residue at positon 167. However, in the work published by Bryan, et al, and also the sequence returned to us by SeqWright DNA Technology Servicess, there should be an alanine residue located at position 166, a lysine residue located at position 167, and the extra amino acid, proline, located at position 168. Although there are differences between the two sequences, the gene is transcribed correctly into RNA resulting in a complete, correct translation into protein.

The sequence of *mmgB* is not attributed to its inactivity, because the nucleic acid sequence is still in frame with the promoter. However, there is still the possibility that the His_6 tag located on the C-terminus of the protein may be interfering with its activity.

Figure 23. DNA sequence alignment of the *mmgB* gene. The lower case sequence is from the Subtilist web server. The upper-case sequence is from the NCBI data bank, accession number U29084.

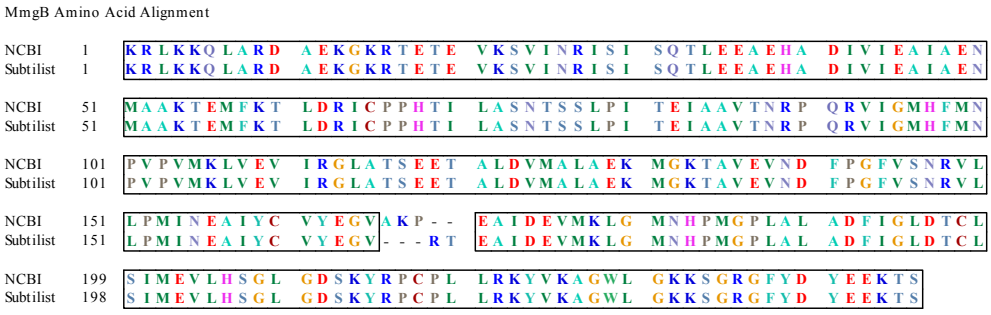

Figure 24. Amino Acid Alignment. The amino acid alignment of MmgB from NCBI accession number U29084 and the Subtilist web server.

II.C Experimental Section

II.C.1 MmgC/B Amplification

To isolate *B. subtilis* 168 DNA, BS168 cells were streaked onto an LB plate and incubated overnight at 37 ^{0}C. A starter culture was then made by inoculating 5 mL of LB with one colony of BS168. The Wizard® Genomic DNA Purification Kit, manufactured by Promega, was then used to isolate the BS168 genomic DNA. In order to amplify the genes of interest, primers were designed for the *mmgC* and *mmgB* gene.

The upstream primer designed for *mmgC* was 5'-GGG GTG GCC CAT ATG CAT GTA AC- 3' (*Nde*I restriction site) and the downstream primer was 5'- CGT TTT TCT CGA GTC AGG TTC CGC -3' (*Xho*I restriction site). For *mmgB*, the upstream primer was 5'-GCA GCC ATG GAA CGG CTG AAG- 3' (*Nco*I restriction site) and the downstream primer was 5'- AAT AGC TCG AGG GAA GTC TTC TCC TCA TAG -3' (*Xho*I restriction site). The primers were manufactured by Integrated DNA Technologies, Coralville, IA. A high-fidelity polymerase chain reaction (PCR) kit, manufactured by Finnzymes Oy, was then used to amplify *mmgC/B* in a thermocycler. The reaction was started with an initial incubation at 98.0 ^{0}C for 30 seconds, followed by 30 cycles of denaturing at 98.0 ^{0}C for 10 seconds, annealing for 30 seconds at 63.4 ^{0}C for *mmgC* and 63.0 for *mmgB*, and extension at 72.0 ^{0}C for 30 seconds. After thirty cycles the reaction mixture was held constant at 4.0 ^{0}C.

In order to determine that the polymerase chain reaction (PCR) amplification was successful, the PCR products were analyzed by 0.7 % agarose gel electrophoresis. The

QIAquick PCR Purification Kit, manufactured by QIAGEN (cat no. 28104) was then used to purify the PCR products.

II.C.2 MmgC/B Cloning

The QIAprep® Spin Miniprep Kit, manufactured by QIAGEN Sciences, was used to purify pET-28a plasmid from transformed DH5α/pET28a cells. A restriction digest was then performed on the PCR products and purified pET28a plasmid. The restriction enzymes *Xho*I and *Nde*I were used for *mmgC* and pET28a. The restriction enzymes *Xho*I and *Nco*I were used for *mmgB* and pET28a. The restriction enzymes were manufactured by New England BioLabs. A low temperature agarose gel was then used to separate the components of the reaction mixture. The desired fragments (*mmgC/B* and pET28a containing) were then cut from the gel and melted at 75 ^{0}C. The genes were then ligated into the pET28a vector with T4 DNA ligase in a thermocycler. The ligation reaction temperatures were set at 37.0 ^{0}C for 30 minutes, then 23.0 ^{0}C for 2 hours 30 minutes, and finally held at 16.0 ^{0}C overnight.

After successful ligation of the *mmgC*/pET-28a and *mmgB*/pET-28a systems, DH5α cells were transformed with the ligated products. The transformed cells were then plated onto agar containing kanamycin (30 mg/L) and incubated overnight at 37 ^{0}C. Each resulting colony was then used to inoculate 5 mL of LB containing kanamycin (30 mg/L). The plasmids from these colonies were purified and a PCR reaction was run on each sample.

Having successfully ligated the genes of interest with pET28a expression vectors, the *mmg*C/pET-28a and *mmgB*/pET-28a expression vectors needed to be introduced into

an appropriate expression host. To do that, *E. coli* cells, of the strain BL21(DE3), were swabbed onto a Luria-Burtani (LB) plate. The plate was then incubated overnight at 37 ^{0}C. The cells from one colony were then added to 5 mL of LB and grown overnight at 37 ^{0}C. Two hundred micro-liters of this cell culture was then added to 5 mL of LB. The sample was shaken until cloudy and then subjected to centrifugation at top speed in a clinical centrifuge. The supernatant was discarded and the remaining cells were resuspended in 3 mL of cold 50 mM $CaCl_2$ and vortexed briefly. The resuspension was incubated in ice for 30 minutes. The sample was then centrifuged for 5 minutes at top speed in a clinical centrifuge and the supernatant was discarded. The cellular pellet was then resuspended in 1 mL of cold $CaCl_2$ (50 mM). One hundred micro-liters of competent cells were then mixed with 1 µL of suspended plasmid and incubated on ice for 30 minutes. The sample was then incubated at 37 ^{0}C for 2 minutes and then at room temperature for 10 minutes. One milliliter of LB was then added to the sample and incubated at 37 ^{0}C for 1 hour. The sample was spun at 8,000 rpm for 5 minutes and 1 mL of the supernatant was discarded. The pelleted cells were resuspended and plated onto agar plates containing 30 µg/mL kanamycin and incubated overnight at 37 ^{0}C.

II.C.3 MmgC/B Overexpression and Purification

One starter culture was made by inoculating 5 mL of LB containing 30 µg/mL kanamycin with one colony of *mmgB*/pET28a/BL21(DE3) and *mmgC*/pET28a/BL21(DE3), separately. The cultures were incubated overnight at 37 ^{0}C. Two milliliters of the starter culture were then used to inoculate 1 L of LB containing 30 µg/mL kanamycin and allowed to grow at 37 ^{0}C until their optical density at 595 nm

(OD_{595}) reached 0.5, (OD_{595} = 0.5). Isopropyl-ß-D-thiogalactopyranoside (IPTG) was then added to a final concentration of 1 mM in order to induce *mmgC/B* production. The *mmgC*/pET28a/BL21(DE3) culture was incubated overnight at 37 ^{0}C and the *mmgB*/pET28a/BL21(DE3) was incubated overnight at 18 ^{0}C. During growth, samples were collected every hour for three hours and once after an overnight incubation. A 10 % SDS gel was run to check for increased protein concentration as a function of incubation time.

The cells from the overnight cultures were harvested by centrifugation (6000 g, 10 minutes.) The cells were then resuspended in binding buffer (5 mM imidazole, 500 mM NaCl, 20 mM Tris·HCl, pH 7.9) and lysed by sonication on ice for 3 minutes. The lysate was cleared by centrifugation (11000 g, 30 minutes.) The lysate was then syringe filtered through a 0.45 micron syringe filter (Corning®) and applied to a nickel-nitrilotriacetic acid (Ni-NTA) column. Proteins without the His_6-tag were removed using wash buffer (60 mM imidazole, 500 mM NaCl, 20 mM Tris·HCl, pH 7.9) and MmgC/B was eluted from the column with elution buffer (200 mM imidazole, 500 mM NaCl, 20 mM Tris·HCl, pH 7.9). The methods of Bradford were then used to determine the amount of purified protein from each sample.[47] The MmgC/B eluent was subject to buffer exchange by repeated dilution/concentration cycles with 50 mM Tris·HCl, 20 mM Mg_2Cl at pH 8.0. MmgC/B was concentrated using Amicon centriprep 3 filtration units. SDS-PAGE was run on the concentrated samples to check for purity and integrity. Glycerol was then added to the protein sample to a final concentration of 10 % and the protein was stored at -80 ^{0}C.

II.C.4 Matrix Assisted Laser Desorption Ionization - Time of Flight - Mass Spectrometry

Matrix assisted laser desorption ionization – time of flight – mass spectrometry (MALDI-TOF-MS) was used in the analysis of CoA and its derivatives and also for the analysis of coenzyme presence in the purified protein. The MALDI-TOF-MS instrument used was a 4700 Proteomic Analyzer, made by Applied Biosystems. The samples were analyzed using MS reflector positive ion mode with a fixed laser intensity of 3751.

The sample matrix consisted of 10 mg of 2,5-dihydroxybenzoic acid dissolved in 1 mL of matrix A diluent (50 % acetonitrile in 0.3 % trifluoroacetic acid.) Unless otherwise noted, all samples were prepared by making a 50:50 mixture of sample:matrix, where 0.5 μL was spotted onto the sample plate and allowed to air dry.

II.C.5 Determination of Coenzyme Presence in MmgC and MmgB

Previous MmgB and MmgC samples that had precipitated out of solution were subject to MALDI-TOF-MS analysis in order to determine if any coenzyme may have coeluted during purification. Also, 290 μM samples of FAD(H), FMN, NAD(H), and NADP(H) were ran individually as standards.

II.C.6 MmgC Activity Determination

A reaction mixture was made containing 1.5 mM phenazine methosulfate (PMS), 48 uM 2,6-dichloroindophenol (DCPIP), 33 uM butyryl-CoA, and MmgC. Product formation was monitored using MALDI-TOF analysis. High performance liquid chromatography (HPLC) was also used to confirm product formation. A Varian Prostar HPLC instrument equipped with a 150 x 3.9 mm Waters NovaPak C18 reversed phase

column with a 4 μM particle size was used. An isocratic method of 95% of 200 mM ammonium actetate, pH 6.0, and 5% acetonitrile was run at 1 mL/min and the absorbance was monitored at 261 nm. However, PMS and the CoA derivatives being studied had similar retention times. In order to avoid the interfering peak caused by PMS, ferricenium hexafluorophosphate ($Fc^+PF_6^-$) ion was used as the terminal electron acceptor for the reaction and replaced both DCPIP and PMS.[30] Fresh ferricenium hexafluorophosphate solution was prepared by dissolving the salt in 10mM HCl and standardizing it spectrophotometrically at 617 nm using 617 $M^{-1}cm^{-1}$ as the extinction coefficient.[31] The modified MmgC reaction mixture contained 200 μM butyryl-CoA, 450 μM ferricenium hexafluorophosphate, and 6.94 μM MmgC. A fresh solution of this reaction mixture was analyzed using HPLC under the same conditions described above.

II.C.7 MmgC Kinetic Analysis

Reactions were prepared with 500 μM $Fc^+PF_6^-$, 50 μM MmgC, and varying concentrations of butyryl-CoA. The reaction mixture was brought to 500 μL using 50 mM Tris / 20 mM $MgCl_2$ buffer at a pH = 8. MmgC activity was followed by the decrease in absorbance at 300 nm as the ferricenium ion ($\Delta\varepsilon$ = 4300 $M^{-1}cm^{-1}$)[30] was reduced. The reaction was monitored using a CARY 100 BIO, UV-visible spectrophotometer set at a wavelength of 300 nm.

The substrate tolerance of MmgC to propionyl-CoA, isobutyryl-CoA, and isovaleryl-CoA was monitored by looking for product formation using MALDI-TOF-MS. Reaction mixtures were made in 50 mM Tris / 20 mM $MgCl_2$ buffer at a pH = 8 and contained 500 μM $Fc^+PF_6^-$, 68 μM MmgC and 290 μM acyl-Coenzyme A derivative.

II.C.8 MmgB Activity Determination

Reaction mixtures were made containing 290 μM NAD^+, 290 μM D, L-3-hydroxybutyryl-CoA and MmgB in the buffers listed in Table 1. MALDI-TOF-MS analysis was used to observe product formation.

Table 1. MmgB Buffers

MmgB Reaction Buffers	
Buffer	**pH**
50 mM Tris	9
100 mM KPi (Potassium Phosphate)	6
100 mM KPi	6.4
100 mM KPi	7
100 mM KPi	7.4
100 mM KPi	8
50 mM Tris / 150 mM KCl	6
50 mM Tris / 150 mM KCl	8
50 mM Tris / 150 mM KCl	9
50 mM Tris / 20 mM MgCl2	8

Two different reaction mixtures were also made and analyzed using MALDI-TOF-MS after a 1 hour incubation at room temperature and after a 7 hour incubation at room temperature. The first contained 200 μM HB-CoA, 200 uM NADPH, and MmgB in 50 mM Tris / 20 mM $MgCl_2$ at pH = 8.0 buffer. The second reaction mixture was made to contain 200 uM Acac-CoA, 200 uM $NADP^+$, and MmgB in 50 mM Tris / 20 mM $MgCl_2$ at pH = 8.0 buffer.

In case of isomer inhibition, analysis of reactions containing enantiopure substrate was also performed. In 50 mM potassium phosphate buffer (pH 6 and 7) and in 50 mM Tris buffer (pH 8 and 9), 4.8 μL of MmgB, 200 μM $NADP^+$, and 2 μL of enantiopure

substrate (concentration unknown) was added. After a 30 minute incubation at room temperature the samples were subjected to MALDI-TOF-MS analysis.

In 100 µL of Tris buffer (pH = 9), 10 µL of MmgB, 10 uL of enantiopure HB-CoA, and either 200 µM $NADP^+$ or NAD^+ was added. After a 30 minute and overnight incubation at room temperature, the samples were subjected to MALDI-TOF-MS analysis.

II.C.9 MmgB Sequencing

pET28a/*mmgB* plasmid was purified from host BL21(DE3) cells using the QIAquick MiniPrep Kit, manufactured by QIAGEN. The plasmid was then retransformed into DH5α using previously described methods. Plasmid was then purified from an overnight culture of *mmgB*/DH5α using the QIAquick MiniPrep Kit. The plasmid was diluted to 250 µg/mL and sent to SeqWright DNA Technology Services, Houston, TX for sequencing.

II.C.10 (S)- and (R)-β-Hydroxybutyryl-CoenzymeA Synthesis

(*S*)- and (*R*)-β-hydroxybutyryl-coenzymeA (HB-CoA) synthesis was done following the work of Yuan, et al.[48] The enantiopure synthesis of (*S*) and (*R*)-β-hydroxybutyryl-CoA was carried out separately using the same procedure. To 4 mL of dry dimethlyformamide (DMF), 1.3 g of tert-butyldimethyl silyl chloride (TBDMSCl) was added. Under argon and on ice, 1.7 grams of imidazole was added and dissolved. Two hundred fifty milligrams of enantio-pure β-hydroxybutyric acid (Sigma) was dissolved in 1 mL of dry DMF and added to the reaction. The reaction was warmed to room temperature and stirred overnight. The mixture was poured over 30 mL of

saturated NaCl and extracted with a 1:3 mixture of ether:petroleum ether (5 x 15 mL). The mixture was dried over $MgSO_4$, filtered, and the filtrate was concentrated under reduced pressure. The residue was dissolved in 30 mL methanol and 15 mL THF. Seven hundred fifty milligrams potassium carbonate dissolved in 5 mL water was added and the reaction was stirred overnight at room temperature. To the reaction, 10 mL of saturated NaCl was added and the pH was adjusted to 3 with 1 M H_2SO_4. The solution was then extracted (5 x 10 mL) with a 1:3 ether: petroleum ether mixture. The organic layers were combined, dried over $MgSO_4$, and filtered. The solvent was removed under reduced pressure overnight. The remaining residue was dissolved in 5 mL of CH_2Cl_2. Under argon, at 0 ^{0}C, 1 equivalent of dicyclohexylcarbodiimide (DCC) and 1 equivalent of benzenethiol was added, warmed to room temperature, and stirred overnight. Fifteen milliliters of ether was added and the precipitate was removed by filtration. The solvent was removed under reduced pressure. The residue was then purified by flash chromatography (5% ethyl acetate in hexanes) and the solvent was removed under reduced pressure. The remaining residue was dissolved in 2 mL of acetonitrile and 5 mL of 5% HF in acetonitrile was added. When the reaction ceased, as monitored by thin layer chromatography (TLC), saturated $NaHCO_3$ was added until the evolution of CO_2 ceased. The mixture was then extracted with ether (3 x 20 mL). The organic layers were combined, washed with NaCl, and dried over $MgSO_4$. The solvent was removed under reduced pressure. To 0.250 mL of a 50 mM solution of potassium phosphate buffer, pH = 7.8, saturated with argon, 10 mg of CoA dissolve in 100 µL acetonitrile was added. The reaction was stirred vigorously overnight. One hundred microliters of water was

added and the mixture was extracted with ether (5 x 3 mL). The aqueous layer was further purified with HPLC. For HPLC, one hundred microliters of the sample was dissolved in 100 μL of 95% ammonium acetate buffer (pH 6.5) and 5% acetonitrile. The sample was syringe filtered (45 μm) and HPLC was run isocratically with 95% ammonium acetate buffer, pH 6.5, and 5% acetonitrile. The peaks from five 10 μL injections of sample from above were collected and pooled. The collected sample was lyophilized, diluted with 2 mL water and lyophilized again to remove ammonium acetate. MALDI-TOF-MS analysis was run on each sample.

II.D Conclusion

MmgC and MmgB from *Bacillus subtilis* strain 168 were successfully cloned into pET-28a plasmid and transformed into *E. coli* strain BL21(DE3). IPTG was successfully used to induce MmgC/B transcription and translation. Because of the C-terminal His_6-tag attached from its insertion into pET-28a, MmgC was purified using a Ni-NTA column. Likewise, an N-terminal His_6-tag on MmgB allowed for its purification using a Ni-NTA column.

MALDI-TOF-MS analysis confirmed that FAD was present in MmgC and NADP in MmgB. Because of their presence, it is presumed that they are coenzymes and act as the oxidizing agents for the catalyzed reactions.

The activity of MmgC was determined spectrophotometrically by HPLC and MALDI-TOF-MS analysis. During HPLC, the presence of the coenzyme A derivative used in the assay was monitored at 261 nm. Using butyryl-CoA and butenoyl-CoA as standards for the determination of the retention times of reactants and products, it was

confirmed that the purified protein was, in fact, active and able to catalyze the conversion of butyryl-CoA to butenoyl-CoA. This reaction was also confirmed using MALDI-TOF-MS analysis using the same standards and under the same reaction conditions.

The activity and also the selectivity of MmgC have been confirmed by HPLC and MALDI-TOF-MS analysis towards butyryl-, isobutyryl-, propionyl-, and isovalyryl-CoA. MmgC is able to catalyze the conversion of butyryl-CoA to butenoyl-CoA and isobutyryl-CoA to isobutenoyl-CoA. On the other hand, MmgC was not able to catalyze the conversion of propionyl-CoA to acrolyl-CoA or isovaleryl-CoA to 3-methylcrotonyl-CoA.

This is consistent with the expected metabolic pathway involving MmgC. Butenoyl-CoA can be further broken down into acetyl-CoA by the rest of the enzymes in the β-oxidation pathway of fatty acid metabolism. The resulting isobutenoyl-CoA, from isobutyryl-CoA, can be further metabolized into acetyl-CoA and propionyl-CoA. Propionyl-CoA can then enter the methylcitric aid cycle. The fact that propionyl-CoA would enter the methylcitric acid cycle explains why it is not likely oxidized by MmgC to produce acrolyl-CoA. If isovaleryl-CoA were oxidized by MmgC, the product would be 3-methylcrotonyl-CoA. If 3-methylcrotonyl-CoA were to follow the pathway of β-oxidation, the next step would be hydration across the double bond at position three. However, oxidation cannot occur on a tertiary alcohol. Therefore, this substrate is not suitable for the β-oxidation pathway.

One other substrate that can logically be broken down through the β-oxidation pathway is 2-methylbutyryl-CoA; the expected penultimate product of anteiso fatty acid

β-oxidation. The resulting product from the MmgC reaction would be 2-methylbutenoyl-CoA which would ultimately be degraded into acetyl-CoA and propionyl-CoA. However, this reaction was not studied because this substrate is not commercially available. For a later study of this reaction, the synthesis of 2-methylbutyryl-CoA is being attempted by another colleague, Hussam Hamoush, following a modified procedure of the HB-CoA synthesis described earlier.

Monitoring the reduction of the ferricenium ion during catalysis, the kinetic rate constants, K_m, V_{max}, and k_{cat} were calculated for MmgC. The calculated values show that MmgC prefers isobutyryl-CoA over butyryl-CoA as substrate. As determined by the k_{cat}/K_M value, MmgC is about 2.5 fold more efficient at catalyzing the reaction of isobutyryl-CoA to isobutenoyl-CoA than it is at catalyzing the reaction of butyryl-CoA to butenoyl-CoA. Because the membranes of *B. subtilis* contain a significant amount of branched chain fatty acids in the form of phospholipids and that it can be proposed that *B. subtilis* is metabolizing these phospholipids for the generation of energy during sporulation, it makes sense that there would be an acyl-CoA dehydrogenase that shows a higher specificity toward branched chains.

MmgC is an enzyme that can catalyze the oxidation of an acyl-CoA to form an enoyl-CoA. This is particularly important when *B. subtilis* is undergoing sporulation and in need of energy. During the catalytic conversion of reactant to product, one equivalent of $FADH_2$ is also produced. The electrons given to FAD to produce $FADH_2$ are subsequently used for the production of two ATP molecules. The newly synthesized

enoyl-CoA continues through the pathway of the β-oxidation of fatty acid metabolism producing more energy for the sporulating *B. subtilis.*

The gene *yngF*, also controlled by σ^E, shows sequence similarity to 3-hydroxybutyryl-CoA dehydratase and may be responsible for the hydration of the enoyl-CoA to produce a β-hydroxyacyl-CoA.[24] If this is true, this gene could be responsible for the next step in the β-oxidation of fatty acids. Currently, this hypothesis is being tested by Jeffrey Smith at The University of North Carolina at Greensboro.

Although not confirmed in this study, MmgB may then be responsible for the dehydrogenation of the β-hydroxyacyl-CoA to form acetoacetyl-CoA. However, MmgB showed no catalytic activity towards D- or L-β- hydroxybutyryl-CoA. Although there is conflict between the amino acid sequences from Bryan, et al, and the Subtilist genome project, the differences do not appear to be significant enough to affect the activity of the enzyme. Therefore, the lack of activity for this enzyme must be further investigated to gain full understanding of the role of this gene during sporulation.

Two hypotheses as to why there is no observed activity can be argued. The first hypothesis is that the presence of the C-terminal histidine-tag on MmgB may be interfering with its activity. The second hypothesis is that 3-hydroxybutyryl-CoA may not be the correct substrate for MmgB.

In order to test whether the His_6-tag is interfering with activity, the histidine-tag can be moved from the C-terminus to the N-terminus of the polypeptide sequence. In order to do this, new primers could be designed to incorporate *Nde*I and *Xho*I restriction sites. This will allow for the cloning into the pET28a vector with the histidine-tag

located at the 5' end of the DNA sequence. Furthermore, because the pET28a vector contains a thrombin recognition site directly upstream from the *Nde*I restriction site (Figure 25[49]), the histidine-tag could be removed upon treatment with thrombin.

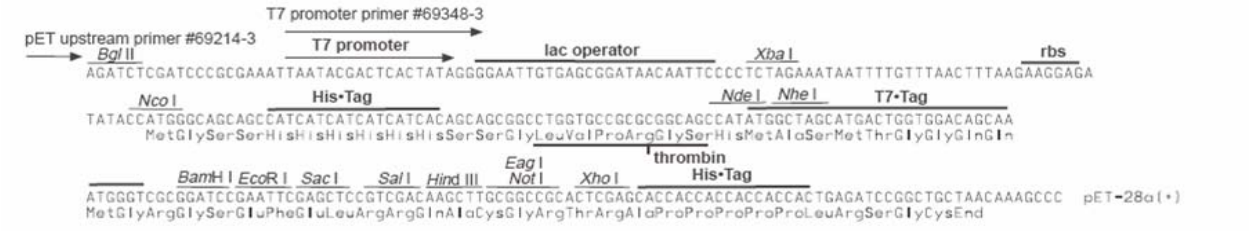

Figure 25. pET-28a(+) Vector Map

Based on the operon in which *mmgB* is located and the data already collected for MmgA[15] and MmgC, it does not seem plausible that 3-hydroxybutyryl-CoA would not be recognized by MmgB. However, if the relocation and/or removal of the histidine-tag does not show activity, alternative substrates could be used to test for enzyme activity. In order to test the hypothesis that 3-hydroxybutyryl-CoA is the wrong substrate, different substrates could be used, including, but not limited to, substrates of longer chain length and branched substrates. The new substrates could include a medium and long chain 3-hydroxyacyl-CoA and also methyl-branched 3-hydroxyacyl-CoAs. These substrates are not commercially available and would need to be synthesized.

Once the activity of MmgB has been established, its kinetic parameters, K_m and V_{max} could be measured by following an increase in absorbance at 340 nm as $NAD(P)^+$ is reduced to NAD(P)H. After K_m and V_{max} have been determined, MmgB's specificity for different substrates could be determined. Also, size exclusion chromatography could be

used to determine if any protein-protein complex formation is occurring between different Mmg proteins.

Biochemically characterizing *mmgC* as an acyl-CoA dehydrogenase has provided one more piece of information that allows for the understanding of energy production in sporulating *B. subtilis*. Likewise, it still seems plausible that MmgB may act as a β-hydroxyacyl-CoA dehydrogenase based on our initial investigation of sequence similarity and cofactor presence. With the biochemical characterization of *mmgC*, *mmgA*[15], and our initial results for *mmgB*, a strong argument can be made that the σ^E dependent *mmg* operon is used for energy production in sporulating *Bacillus subtilis*.

REFERENCES

1. Kunst, F.; Ogasawara, N.; Moszer, I.; Albertini, A. M.; Alloni, G.; Azevedo, V.; Bertero, M. G.; Bessieres, P.; Bolotin, A.; Borchert, S.; Borriss, R.; Boursier, L.; Brans, A.; Braun, M.; Brignell, S. C.; Bron, S.; Brouillet, S.; Bruschi, C. V.; Caldwell, B.; Capuano, V.; Carter, N. M.; Choi, S. K.; Codani, J. J.; Connerton, I. F.; Cummings, N. J.; Daniel, R. A.; Denizot, F.; Devine, K. M.; Dusterhoft, A.; Ehrlich, S. D.; Emmerson, P. T.; Entian, K. D.; Errington, J.; Fabret, C.; Ferrari, E.; Foulger, D.; Fritz, C.; Fujita, M.; Fujita, Y.; Fuma, S.; Galizzi, A.; Galleron, N.; Ghim, S. Y.; Glaser, P.; Goffeau, A.; Golightly, E. J.; Grandi, G.; Guiseppi, G.; Guy, B. J.; Haga, K.; et al., The complete genome sequence of the gram-positive bacterium *Bacillus subtilis*. *Nature (London)* **1997,** *390*, (6657), 249-256.

2. Stephens, C., Bacterial sporulation: A question of commitment? *Current Biology* **1998,** *8*, (2), R45-R48.

3. Stragier, P.; Losick, R., Molecular genetics of sporulation in *Bacillus subtilis*. *Annual Review of Genetics* **1996,** *30*, 297-341.

4. Hilbert, D. W.; Piggot, P. J., Compartmentalization of Gene Expression during *Bacillus subtilis* Spore Formation. *Microbiology and Molecular Biology Reviews* **2004,** *68*, (2), 234-262.

5. Yang, X.; Lewis, P. J., Overproduction and purification of recombinant *Bacillus subtilis* RNA polymerase. *Protein Expression and Purification* **2008***, 59,* (1), 86-93.

6. Burgess, R. R., Separation and Characterization of the Subunits of Ribonucleic Acid Polymerase. *Journal of Biological Chemistry* **1969,** *244*, (22), 6168-6176.

7. Burgess, R. R.; Travers, A. A.; Dunn, J. J.; Bautz, E. K. F., Factor Stimulating Transcription by RNA Polymerase. *Nature* **1969,** *221*, (5175), 43-46.

8. Errington, J., Regulation of endospore formation in Bacillus subtilis. *Nat Rev Micro* **2003,** *1*, (2), 117-126.

9. Kroos, L.; Zhang, B.; Ichikawa, H.; Yu, Y.-T. N., Control of σf factor activity during *Bacillus subtilis* sporulation. *Molecular Microbiology* **1999,** *31*, (5), 1285-1294.

10. Fujita, M.; Sadaie, Y., Rapid isolation of RNA polymerase from sporulating cells of *Bacillus subtilis*. *Gene* **1998,** *221*, (2), 185-190.

11. Pogliano, K.; Hofmeister, A. E.; Losick, R., Disappearance of the sigma E transcription factor from the forespore and the SpoIIE phosphatase from the mother cell contributes to establishment of cell-specific gene expression during sporulation in *Bacillus subtilis*. *Inorg. Chem*. **1997,** *179*, (10), 3331-3341.

12. LaBell, T. L.; Trempy, J. E.; Haldenwang, W. G., Sporulation-Specific sigma Factor sigma 29 of *Bacillus subtilis* is Synthesized from a Precursor Protein, P31. *Proceedings of the National Academy of Sciences* **1987,** *84*, (7), 1784-1788.

13. Bryan, E. M.; Beall, B. W.; Moran, C. P., Jr., A sigma E dependent operon subject to catabolite repression during sporulation in *Bacillus subtilis*. *Journal of Bacteriology* **1996,** *178*, (16), 4778-4786.

14. Eichenberger, P.; Jensen, S. T.; Conlon, E. M.; van Ooij, C.; Silvaggi, J.; Gonzalez-Pastor, J.-E.; Fujita, M.; Ben-Yehuda, S.; Stragier, P.; Liu, J. S.; Losick, R., The [sigma]E Regulon and the Identification of Additional Sporulation Genes in *Bacillus subtilis*. *Journal of Molecular Biology* **2003,** *327*, (5), 945-972.

15. Reddick, J. J., Williams, J.K., The mmgA gene from *Bacillus subtilis* encodes a degradative acetoacetyl-CoA thiolase. *Biotechnology Letters* **2008**, *30*, (6), 1045-1050.

16. Kaneda, T., Fatty Acids of the Genus *Bacillus*: an Example of Branched-Chain Preference. *Bacteriological Reviews* **1977,** *41*, (2), 391-418.

17. Kaneda, T., Iso- and Anteiso-Fatty Acids in Bacteria: Biosynthesis, Function, and Taxonomic Significance. *Bacteriological Reviews* **1991,** *55*, (2), 288-302.

18. Kaneda, T., Biosynthesis of Branched Chain Fatty Acids. I. Isolation and identification of fatty acids from *Bacillus subtilis* (ATCC 7059). *Journal of Biological Chemistry* **1963,** *238*, (4), 1222-1228.

19. Saito, K., Chromatographic studies on bacterial fatty acids. *Journal of Biochemistry* **1960,** *47*, (6), 699-719.

20. Tabuchi, T., Serizawa, N. & Uchiyama, H., A novel pathway for the partial oxidation of propionyl-CoA to pyruvate via seven-carbon tricarboxylic acids in yeast. *Agric. Biol. Chem.* **1974,** *38*, 2571-2572.

21. Brock, M.; Fischer, R.; Linder, D.; Buckel, W., Methylcitrate synthase from *Aspergillus nidulans*: implications for propionate as an antifungal agent. *Molecular Microbiology* **2000,** *35*, (5), 961-973.

22. Brock, M.; Darley, D.; Textor, S.; Buckel, W., 2-Methylisocitrate lyases from the bacterium *Escherichia coli* and the filamentous fungus *Aspergillus nidulans*. *European Journal of Biochemistry* **2001,** *268*, (12), 3577-3586.

23. Koburger, T. W., Jimena; Bernhardt, Joerg; Homuth, Georg; Hecker, M. , Genome-wide mRNA profiling in glucose starved *Bacillus subtilis* cells. *Molecular Genetics and Genomics* **2005,** *274*, (1), 1-12.

24. Subtilist World-Wide Web Server. In 2001.

25. Novagen, pET System Manual. **11th Edition**.

26. Qiagen, The Qiaexpressionist™. *5th ed.*

27. Zeng, J.; Li, D., Expression and purification of His-tagged rat mitochondrial medium-chain acyl-CoA dehydrogenase wild-type and Arg256 mutant proteins. *Protein Expression and Purification* **2004,** *37*, (2), 472-478.

28. Lehman, T. C.; Thorpe, C., Alternate electron acceptors for medium-chain acyl-CoA dehydrogenase: use of ferricenium salts. *Biochemistry* **1990,** *29*, (47), 10594-10602.

29. Zeng, J.; Liu, Y.; Wu, L.; Li, D., Mutation of Tyr375 to Lys375 allows medium-chain acyl-CoA dehydrogenase to acquire acyl-CoA oxidase activity. *Biochimica et Biophysica Acta (BBA) - Proteins & Proteomics* **2007,** *1774*, (12), 1628-1634.

30. Lehman, T. C.; Hale, D. E.; Bhala, A.; Thorpe, C., An acyl-coenzyme A dehydrogenase assay utilizing the ferricenium ion. *Analytical Biochemistry* **1990,** *186*, (2), 280-284.

31. Carney, M. J.; Lesniak, J. S.; Likar, M. D.; Pladziewicz, J. R., Ferrocene derivatives as metalloprotein redox probes: electron-transfer reactions of ferrocene and ferricenium ion derivatives with cytochrome c. *Journal of the American Chemical Society* **1984,** *106*, (9), 2565-2569.

32. Pladziewicz, J. R.; Brenner, M. S., Partitioning of ferrocenium ions between multiple redox sites on spinach plastocyanin. **1987,** *26*, (21), 3629-3634.

33. Maggio-Hall, L. A.; Lyne, P.; Wolff, J. A.; Keller, N. P., A single acyl-CoA dehydrogenase is required for catabolism of isoleucine, valine and short-chain fatty acids in *Aspergillus nidulans*. *Fungal Genetics and Biology* **2008,** *45*, (3), 180-189.

34. Colby, G. D.; Chen, J. S., Purification and properties of 3-hydroxybutyryl-coenzyme A dehydrogenase from *Clostridium beijerinckii* NRRL B593. *Applied and Environmental Microbiology* **1992,** *58*, (10), 3297-3302.

35. Oppermann, U. C. T.; Salim, S.; Tjernberg, L. O.; Terenius, L.; Jornvall, H., Binding of amyloid [beta]-peptide to mitochondrial hydroxyacyl-CoA dehydrogenase (ERAB): regulation of an SDR enzyme activity with implications for apoptosis in Alzheimer's disease. *FEBS Letters* **1999,** *451*, (3), 238-242.

36. Luo, M. J.; Mao, L. F.; Schulz, H., Short-Chain 3-Hydroxy-2-methylacyl-CoA Dehydrogenase from Rat Liver: Purification and Characterization of a Novel Enzyme of Isoleucine Metabolism. *Archives of Biochemistry and Biophysics* **1995,** *321*, (1), 214-220.

37. Haywood, G. W.; Anderson, A. J.; Chu, L.; Dawes, E. A., The role of NADH- and NADPH-linked acetoacetyl-CoA reductases in the poly-3-hydroxybutyrate synthesizing organism *Alcaligenes eutrophus*. *FEMS Microbiology Letters* **1988,** *52*, (3), 259-264.

38. Madan, V. K.; Hillmer, P.; Gottschalk, G., Purification and Properties of NADP-Dependent l(+)-3-Hydroxybutyryl-CoA Dehydrogenase from *Clostridium kluyveri*. *European Journal of Biochemistry* **1973,** *32*, (1), 51-56.

39. He, X. Y.; Yang, S. Y., Histidine-450 Is the Catalytic Residue of L-3-Hydroxyacyl Coenzyme A Dehydrogenase Associated with the Large α-Subunit of the Multienzyme Complex of Fatty Acid Oxidation from *Escherichia coli*. *Biochemistry* **1996,** *35*, (29), 9625-9630.

40. Wakil, S. J.; Bressler, R., Studies on the Mechanism of Fatty Acid Synthesis. X. Reduced Triphosphopyridine Nucleotide-Acetoacetyl Coenzyme A Reductaser. *Journal of Biological Chemistry* **1962**, *237*, (3), 687-693.

41. G. A. F. Ritchie, P. J. S., and E. A. Dawes, The purification and characterization of acetoacetyl-coenzyme A reductase from *Azotobacter beijerinckii*. *Biochemical Journal* **1971,** *121*, (2), 309-316.

42. Liu, X.; Chu, X.; Yu, W.; Li, P.; Li, D., Expression and purification of His-tagged rat mitochondrial short-chain 3-hydroxyacyl-CoA dehydrogenase wild-type and Ser137 mutant proteins. *Protein Expression and Purification* **2004,** *37*, (2), 344-351.

43. Youngleson, J. S.; Jones, D. T.; Woods, D. R., Homology between hydroxybutyryl and hydroxyacyl coenzyme A dehydrogenase enzymes from *Clostridium acetobutylicum* fermentation and vertebrate fatty acid beta-oxidation pathways. *Journal of Bacteriology* **1989,** *171*, (12), 6800-6807.

44. Noyes, B. E.; Bradshaw, R. A., l-3-Hydroxyacyl Coenyzme A Dehydrogenase from Pig Heart Muscle. I. Purification and Properties. *Journal of Biological Chemistry* **1973,** *248*, (9), 3052-3059.

45. Brown, A. J., “Enzyme action.” *J. Chem. Soc.* **1902,** *81*, 373-386.

46. Michaelis, L. a. M., M. L., “Kinetik der Invertinwirkung.” *Biochem. Z.* **1913,** *49*, 333–369.

47. Bradford, M. M., A rapid and sensitive method for the quantitation of microgram quantities of protein utilizing the principle of protein-dye binding. *Analytical Biochemistry* **1976,** *72*, (1-2), 248-254.

48. Yuan, W.; Jia, Y.; Tian, J.; Snell, K. D.; Muh, U.; Sinskey, A. J.; Lambalot, R. H.; Walsh, C. T.; Stubbe, J., Class I and III Polyhydroxyalkanoate Synthases from Ralstonia eutropha and Allochromatium vinosum: Characterization and Substrate Specificity Studies. *Archives of Biochemistry and Biophysics* **2001,** *394*, (1), 87-98.

49. Novagen pET-28a-c(+) Vector Map. http://www.emdbiosciences.com/product/TB074 (April 08, 2008).